



Coriolis Effects in Symmetric Top Spectra


by

LLOYD LEE JOHN CIMPRICH

A Thesis

submitted in conformity with the
requirements for the degree of
Master of Science at Brock University

July, 1974



ABSTRACT

The "x-y Coriolis Coupling Theory" as presented by Dilauro and Mills (1966) is reformulated and extended to the determination of Raman intensities. Theoretical Raman and Infrared spectra are computed in order to understand the effects due to this coupling in both types of spectra. Both the Infrared and Raman spectra obtained indicate very real effects due to Coriolis coupling. In some of the cases chosen the computed spectra are grossly different from the normal spectra where coupling is absent. Such large effects can greatly impede the interpretation of experimental results. Theoretical spectra therefore aids in the interpretation of experimental results, as is clearly demonstrated in the results of this work.

ACKNOWLEDGEMENTS

The author is gratefully indebted to Dr. D. W. Lepard for his patient guidance and encouragement throughout the work and in the preparation of this thesis.

The author would like to thank Drs. E. R. Cowley, J. M. Miller and D. C. Moule for valuable comments. In particular, he would like to thank Dr. Moule for facilitating the use of the McMaster computer (CDC 6400) on which all computed spectra in this thesis were produced.

The author would especially like to thank Mrs. J. Cowan for typing various portions of the manuscript.

TO MY PARENTS

TABLE OF CONTENTS

		Page
Chapter I	INTRODUCTION	1
Chapter II	ENERGY THEORY	3
	1 Introduction	3
	2 Rigid Rotor functions	5
	3 Vibrational Functions	10
	4 The Hamiltonian	16
Chapter III	INFRARED AND RAMAN INTENSITY THEORY	27
	1 Introduction	27
	2 Infrared transition moments	29
	3 Raman moments	34
Chapter IV	COMPUTATIONAL DETAILS	42
	1 Introduction	42
	2 Algorithm details	43
	3 Criteria for good comparison between experimental and simulated spectra	47
Chapter V	RESULTS	49
Chapter VI	CONCLUSIONS	69
Appendix I	ℓ -Doubling	70
	BIBLIOGRAPHY AND REFERENCES	71

LIST OF TABLES

		Page
Table I:	Restriction on $\zeta_{k,\ell}^{\alpha}$	18
Table II:	Energy Matrix for $K>0$	24
Table III:	Energy Matrix for $K=0$	25
Table IV:	Infrared Vibrational Matrix Elements	31
Table V:	Infrared Transition Matrix Elements	33
Table VI:	Raman Vibrational Matrix Elements	37
Table VII:	Raman Transition Matrix Elements ($\Delta K=0$)	39
Table VIIa:	" " " " ($\Delta K=\pm 3$)	40
Table VIIb:	" " " " ($\Delta K=\pm 1$)	40
Table IX:	Isotropic Raman Transition Matrix Elements	41

LIST OF FIGURES

Figure 1:	Relation between Space fixed and Molecule Fixed axes	5
Figure 2:	Relation between Spectral Slit Width and Gaussian	45
Figure 3:	ℓ -Doubling	70

LIST OF DIAGRAMS

		Page
Diagram 1	Infrared ν_2 - ν_5 region of CH_3F (simulated and experimental)	52
Diagram 2	Infrared ν_3 - ν_6 region of CH_3F (simulated and experimental)	54
Diagram 3	Infrared ν_2 - ν_5 region of CD_3Cl (simulated)	56
Diagram 4	Raman ν_2 - ν_5 region of CD_3Cl with $\alpha_1^2=1$; $\alpha_0^2 = \alpha_2^2 = 0$ (simulated)	58
Diagram 5	Raman ν_2 - ν_5 region of CD_3Cl with $\alpha_0^2 = \alpha_1^2 = 1, \alpha_2^2 = 0$ (simulated)	60
Diagram 6	Raman ν_2 - ν_5 region of CD_3Cl with $\alpha_0^2 = 1, \alpha_1^2 = -1, \alpha_2^2 = 0$ (simulated)	62
Diagram 7	Raman ν_2 - ν_5 region of CD_3Cl with $\alpha_0^2 = \alpha_1^2 = 0, \alpha_2^2 = 1$ (simulated)	64
Diagram 8	Raman ν_2 - ν_5 region of CD_3Cl with $\alpha_0^2 = 1, \alpha_1^2 = \alpha_2^2 = 0$ (simulated)	66
Diagram 9	Raman ν_2 - ν_5 region of CD_3Cl with $\alpha_0^2 = \alpha_1^2 = \alpha_2^2 = 1$ (simulated)	68

Chapter I

INTRODUCTION

The present work is primarily concerned with the effects of "X - Y Coriolis coupling" in Raman spectra. That is, effects arising due to coupling of degenerate and non-degenerate vibrational co-ordinates through vibrational angular momentum operators in the Hamiltonian which have the symmetry of rotations about the X or Y axes. The specific molecules to be studied are CH_3F and CD_3Cl , both of symmetry C_{3v} . Results for molecules of different symmetry (particularly those with rotational subgroup D_3) are readily derived. In fact many of the results apply to both C_{Nv} and D_N types, restriction to symmetry C_{3v} being invoked only in the determination of transition moments and selection rules.

The original investigations of this effect were carried out by H.H. Nielsen (see for example Rev. Mod. Phys. 23, 90 (1951)) who described the basic energy theory. Subsequently, many workers have considered the effect of such interactions in infrared spectra (see for example Dilauro and Mills (1966)).

Due to the complexity of the theoretical conventions it was felt necessary to reformulate both the energy theory and the infrared intensity theory (given by Dilauro and Mills) as well as to derive the necessary results for Raman intensities. Thus a comparison of our results with those given by Dilauro and Mills for the infrared case would provide some check of our theory. In addition the application of the infrared results, not entirely unambiguously given by Dilauro and Mills would be clarified.

The results of this work take the form of a series of computer simulated spectra and experimental infrared spectra. The simulated spectra are produced by a computer algorithm written during the course of this work. This algorithm is able to produce simulated infrared spectra on a linear absorption scale or Raman spectra on a linear relative probability scale.

Earlier versions of this algorithm failed to reproduce the spectra published by Dilauro and Mills. The most dramatic difficulties appeared in the ν_3 - ν_6 region of CH_3F where the ν_3 parallel band is approximately 70 times as intense as the ν_6 perpendicular band. As a consequence a sample of CH_3F gas was obtained at the National Research Council and new spectra of the ν_2 - ν_5 and ν_3 - ν_6 regions of CH_3F were produced. When the computer algorithm was modified to more properly simulate the convolution of the spectrophotometer, the unexpected discrepancies between our experimental and computed spectra were eliminated.

Simulation of Raman spectra was attempted once the infrared difficulties were eliminated. Due to a lack of suitable experimental spectra, no attempt was made to "fit" our calculated spectra to experiment. Instead the molecule CD_3Cl was chosen and spectra were computed using constants given by Dilauro and Mills. A series of simulations were produced depicting the Raman spectra for various models.

Chapter II

ENERGY THEORY(II-1) Introduction

The molecular Hamiltonian to be considered may be written

$$[1] \quad \bar{H} = (\bar{J}_a - \bar{\Omega}_a)^2 / 2I_a + (\bar{J}_b - \bar{\Omega}_b)^2 / 2I_b + (\bar{J}_c - \bar{\Omega}_c)^2 / 2I_c + 1/2 \sum_k \bar{P}_k^2 + \bar{V}$$

where J_α and Ω_α ($\alpha = a, b, c$) respectively represent the total angular momentum and the internal (vibrational) angular momentum about the molecule fixed axis α , and P_k is the canonical momentum associated with the normal co-ordinate Q_k . This is a simplified version of the more general form given by Wilson, Decius and Cross and others. Reduction from the more general form to equation [1] above involves the following assumptions and conventions (see Wilson, Decius and Cross).

(i) The vibrational potential energy is assumed to have a deep well at the equilibrium position, so that small vibrations may be assumed, and hence the dependence of the moments of inertia, I_α , on normal co-ordinates may be neglected.

(ii) The molecule fixed a, b, c axes are chosen to coincide with the principal axes of inertia.

(iii) Terms involving squares of normal co-ordinates in the inertia tensor are neglected, as a result of (i) above.

Neglecting the vibrational (internal) angular momentum and assuming a "Hookes Law Potential" [1] becomes

$$[2a] \quad \bar{H} = \bar{H}_R + \bar{H}_V$$

$$[2b] \quad \bar{H}_R = \bar{J}_a^2/2I_a + \bar{J}_b^2/2I_b + \bar{J}_c^2/2I_c$$

$$[2c] \quad \bar{H}_V = 1/2 \sum_k (\bar{P}_k^2 + \omega_k^2 \bar{Q}_k^2)$$

In [2] \bar{H}_R represents the energy operator of a rigid rotating body; \bar{H}_V is the vibrational energy operator of a collection of particles with simple harmonic wavefunctions expressed in terms of normal coordinates. Equation [2] separates rotational and vibrational motions, since $[\bar{H}_R, \bar{H}_V] = 0$, and therefore $\psi_{RV} = \psi_R \psi_V$. Thus we are left with the following eigenvalue equations.

$$[3a] \quad \bar{H}_R \Psi_R = E_R \Psi_R$$

$$[3b] \quad \bar{H}_V \Psi_V = E_V \Psi_V$$

For molecules of axial symmetry, two of the moments of inertia are identical. This fact allows simplification of \bar{H}_R by choosing $I_a = I_b$.

Then

$$[4] \quad \bar{H}_R = (\bar{J}^2 - \bar{J}_c^2)/2I_b + \bar{J}_c^2/2I_c$$

where $\bar{J}^2 = \bar{J}_a^2 + \bar{J}_b^2 + \bar{J}_c^2$. The eigenfunctions that one obtains from

[4] above are commonly referred to as "Rigid Rotor Functions".

These functions when multiplied by the simple harmonic oscillator functions form a complete set which is used as the "Basis Set" to write the matrix of the energy operator \bar{H} in [1]. Diagonalization of this matrix yields the energy eigenvalues and their corresponding eigenvector coefficients. The associated wavefunctions are simply those linear combinations of basis set functions obtained by multiplying each such function by its eigenvector coefficient.

(II-2) Rigid Rotor Functions:

These functions have been described by many authors (see for example Wollrab) and require only a brief description here. It is necessary, however, to lay out in detail our particular choice of functions and operators along with their corresponding transformation properties. The latter involves a study of the effect of symmetry transformations on these functions so that we may determine selection rules by means of identifying transitions that are forbidden by symmetry.

The "Rigid Rotor Functions" involve three quantum numbers, J , k , and m . The significance of each quantum number is given below

- J - total angular momentum
- k - component of J along main symmetry axis (molecular top axis "c") of a molecule of axial symmetry.
- m - component of J along the space fixed (lab frame) Z axis.

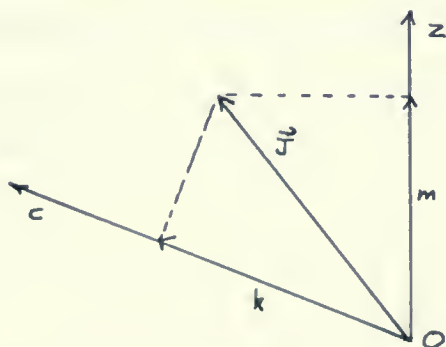


Fig. 1: Relation between space fixed and molecule fixed axes.

A common notation for these functions is $\psi_R = |J,k,m\rangle$ where k and m may take on the usual $2J+1$ values from $-J$ to $+J$.

The particular form of functions and operators used are detailed below

$$[5a] \quad |J,k,m\rangle = C_{J,k,m} (\bar{J}_x - i\bar{J}_y)^{(J-m)} (\bar{J}_a + i\bar{J}_b)^{(J-k)} |J,J,J\rangle^*$$

$$[5b] \quad \bar{J}_x \pm i\bar{J}_y = i\hbar e^{\pm i\phi} (\cot\theta \partial/\partial\phi \mp i \partial/\partial\theta - \csc\theta \partial/\partial\chi)$$

$$[5c] \quad \bar{J}_a \mp i\bar{J}_b = i\hbar e^{\pm i\chi} (\csc\theta \partial/\partial\phi \pm i \partial/\partial\theta - \cot\theta \partial/\partial\chi)$$

$$[5d] \quad |J,J,J\rangle = \sqrt{(2J+1)/8\pi^2} e^{iJ\phi} e^{iJ\chi} [(1/2)(1+\cos\theta)]^J$$

$$[5e] \quad C_{J,k,m} = (1/\hbar)^{(2J-k-m)} \sqrt{((J+k)!(J+m)!)/[(2J)!]^2 (J-m)!(J-k)!}$$

*

$|J,J,J\rangle$ is used as a starting function instead of $|J,0,0\rangle$ used by Hougen (1962) to bypass difficulties of even and odd J values. Note that x,y,z refer to space fixed coordinates and a,b,c refer to molecule fixed coordinates.

It may be noted in passing that [5a] above exhibits the so called "Anomalous Sign of i". The angles θ , ϕ , χ , are the "Euler Angles", as defined in "Appendix I, Wilson, Decius and Cross", which relate the observer's X, Y, Z frame to the molecule fixed a, b, c frame. The operators defined by [5b] and [5c] have the effect of ladder operators on the $|J, k, m\rangle$ functions, incrementing to new functions by raising or lowering the m and k dependence of these functions one unit respectively, according as the upper or lower sign is chosen. In isotropic space the $2J+1$ $|J, k, m\rangle$ functions for a given J and k corresponding to all possible m values will be degenerate. Henceforth they will be denoted $|J, k\rangle$. The determination of transition moments will, however, require a return to the full notation $|J, k, m\rangle$.

The operator defined in [5c] has the following effect on the rotational functions.

$$[6] \quad \bar{J}_{\pm} |J, k\rangle = \sqrt{(J \pm k)(J \mp k + 1)} \hbar |J, k \mp 1\rangle$$

where $\bar{J}_{\pm} = \bar{J}_a \pm i\bar{J}_b$; also we have the usual results

$$[7a] \quad \bar{J}^2 |J, k\rangle = J(J+1) \hbar^2 |J, k\rangle$$

$$[7b] \quad \text{and } \bar{J}_c |J, k\rangle = k \hbar |J, k\rangle$$

Then for molecules of axial symmetry, equation [3a] yields

$$[8] \quad \bar{H}_R |J, k\rangle = [BJ(J+1) + (A-B)k^2] |J, k\rangle$$

where $A = \hbar^2 / 2I_a$; $B = \hbar^2 / 2I_c$.

* For wavenumber units (cm^{-1}) we divide E_R by hc and so obtain

$$A(\text{cm}^{-1}) = A/hc \quad \text{etc.}$$

To complete the description of the "Rigid Rotor Functions" it is necessary to determine their transformation properties under the symmetry operations of the point group concerned. Using the previously given definitions of the functions in terms of Euler Angles (see equation [5]) and using the transformation properties of these angles (appendix I, Wilson, Decius and Cross), the following results are obtained,

$$[9a] \quad (C_N, S_N) |J, k\rangle \rightarrow (e^{i\theta k}, e^{i\theta k(N/2+1)}) |J, k\rangle$$

$$[9b] \quad [C_v \equiv C_{2a} \text{ or } \sigma(bc)] |J, k\rangle \rightarrow (-1)^{-J} |J, -k\rangle$$

$$[9c] \quad [C_{2b} \text{ or } \sigma_v \equiv \sigma(ac)] |J, k\rangle \rightarrow (-1)^{J-k} |J, -k\rangle$$

$$[9d] \quad [C_2 \equiv C_{2c} \text{ or } \sigma_h \equiv \sigma(a \ b)] |J, k\rangle = (-1)^k |J, k\rangle$$

where $\theta = \frac{2\pi}{N}$ used here is not the Euler angle θ previously used in eq [5].

There are two popular schemes for the symmetry classification of rotational functions. The key difference between these two schemes lies in their treatment of improper rotations, which may always be replaced by corresponding proper rotations followed by inversions. Since inversion corresponds to transforming from a right hand system to a left, or vice versa, its effect is not really defined. It is clear, however, that the most that can happen is a change of sign, so that we may label states as - or + according as they do or do not change sign under inversion. The two schemes and how they handle this effect will now be given.

I Hougen Scheme. This scheme does not classify states as + or - due to inversion. The classification of levels is made with respect to the full molecular point group.

II Landau and Lifshitz. For non-planar molecules there are always two levels corresponding to the two possible inversion configurations. These levels are defined as - or + according as they do or do not change sign under inversion. Each level in the former scheme now becomes a degenerate (-,+) pair of levels when inversion splitting is ignored.

The difference between these schemes is actually very minor. The "+" levels in the latter are in reality identical to the former scheme, and the "-" levels are simply specified by changing the sign of the character of the species under improper rotations. There is, however, a conceptual advantage to the latter scheme. That is, the full molecular point group designation may be associated with a distinct nuclear statistical weight and the usual parity selection rules, $\bar{+} \leftrightarrow \pm$ and $\pm \leftrightarrow \pm$ for Infrared and Raman transitions respectively, are obeyed. The Hougen scheme requires selection rules in terms of the full molecular group, and nuclear statistical weights are associated only with a rotational subgroup species instead of the full molecular group species.

(II-3) Vibrational Functions.

The purely vibrational Hamiltonian is

$$[10] \quad \bar{H}_V = 1/2 \sum_k (\bar{P}_k^2 + \omega_k^2 \bar{Q}_k^2)$$

where Q_k is the normal co-ordinate (assumed expressed in terms of mass-weighted Cartesian displacement coordinates) corresponding to the mode ν_k , and P_k is the momentum conjugate to Q_k . For molecules of axial symmetry we may have non-degenerate or doubly degenerate modes.

The non-degenerate modes have the usual "simple harmonic oscillator" form and the following eigenvalue equation

$$[11] \quad \bar{H}_r \Pi_r |v_r\rangle = \hbar [\sum_r (\nu_r + 1/2) \omega_r] \Pi_r |v_r\rangle^*$$

$$\text{where} \quad \bar{H}_r = 1/2 \sum_r (\bar{P}_r^2 + \omega_r^2 \bar{Q}_r^2)$$

Note that "r" runs over all non-degenerate co-ordinates; $|v_r\rangle$ is the eigenfunction corresponding to the normal co-ordinates Q_r and ν_r is the vibrational quantum number.

Considering only one non-degenerate mode, "r" say, we define the operator

$$[12] \quad \bar{R}_r^\pm = \sqrt{1/2} (\bar{P}_r \pm i \omega_r \bar{Q}_r)$$

and following standard methods (Dicke and Wittke, Chapter 6) we obtain the following results:

* For (cm^{-1}) units we divide vibrational energy by hc and so replace $\hbar \omega_r$ by $\nu_r (\text{cm}^{-1}) \equiv \omega_r / 2\pi c$.

$$[13a] \quad |v_r\rangle = 1/\sqrt{(\hbar\omega_r)^{v_r} v_r!} \bar{R}_{r+}^{v_r} |0\rangle$$

$$[13b] \quad \bar{R}_{r+} |v_r\rangle = \sqrt{\hbar\omega_r(v_r+1)} |v_r+1\rangle$$

$$[13c] \quad \bar{R}_{r-} |v_r\rangle = \sqrt{\hbar\omega_r v_r} |v_r-1\rangle$$

$$[13d] \quad \bar{H}_r |v_r\rangle = (v_r+1/2)\hbar\omega_r |v_r\rangle$$

$$[13e] \quad |0\rangle = (\omega_r/\pi\hbar)^{1/4} \exp(-\omega_r Q_r^2/2\hbar)$$

$$[13f] \quad \bar{Q}_r = (-i/\sqrt{2}\omega_r)(\bar{R}_{r+} - \bar{R}_{r-})$$

These provide a sufficiently detailed description of the non-degenerate functions.

The doubly degenerate modes result from two normal co-ordinates which give rise to the same vibrational energy. If we label the two components of the s^{th} degenerate mode as (X_s, Y_s) and their conjugate momenta as (P_{X_s}, P_{Y_s}) respectively, we obtain the following Hamiltonian.

$$[14] \quad \bar{H}_s = (1/2)(\bar{P}_{X_s}^2 + \bar{P}_{Y_s}^2) + (1/2)\omega_s^2(\bar{X}_s^2 + \bar{Y}_s^2)$$

We define the operator \bar{R}_s as follows

$$[15] \quad \bar{R}_s = \bar{R}_{X_s} \hat{a}_{X_s} + \bar{R}_{Y_s} \hat{a}_{Y_s}$$

where $\bar{R}_{X_s} = (1/\sqrt{2})(\bar{P}_{X_s} + i\omega_s \bar{X}_s)$; $\bar{R}_{Y_s} = (1/\sqrt{2})(\bar{P}_{Y_s} + i\omega_s \bar{Y}_s)$

From \bar{R}_{x_s} and \bar{R}_{y_s} we construct the following operators

$$[16a] \quad \bar{R}_{s+} = \bar{R}_{x_s} + i\bar{R}_{y_s} \quad ; \quad \bar{R}_{s-} = \bar{R}_{x_s} - i\bar{R}_{y_s}$$

$$[16b] \quad \bar{Z}_s^{\pm} = \bar{X}_s^{\pm} \mp i\bar{Y}_s \quad \bar{P}_s^{\pm} = \bar{P}_{x_s}^{\pm} \mp i\bar{P}_{y_s}$$

$$= (-i/\sqrt{2}\omega_s)(\bar{R}_{s+} - \bar{R}_{s-}^{\dagger}) ; \quad = (1/\sqrt{2})(\bar{R}_{s+} + \bar{R}_{s-}^{\dagger})$$

Since (X_s, Y_s) are first order Coriolis coupled, the particles will describe an elliptical path about the equilibrium position in the X_s, Y_s plane, loosely speaking. Thus the particles motion will create angular momentum normal to this plane. We shall define \bar{L}_{Z_s} as the operator pertaining to the angular momentum,

$$[17] \quad \bar{L}_{Z_s} = \bar{X}_s \bar{P}_{y_s} - \bar{Y}_s \bar{P}_{x_s}$$

and we shall use l_s to represent the eigenvalue pertaining to \bar{L}_{Z_s} .

Thus for degenerate modes we have functions $|v_s, l_s\rangle$, where v_s is the composite vibrational quantum number, and l_s is the vibrational angular momentum quantum number. These functions can be expressed in terms of the previously given operators as follows.

$$[18a] \quad |v_s, l_s\rangle = C_{v_s, l_s} (\bar{R}_{s-})^{(v_s - l_s)/2} (\bar{R}_{s+})^{(v_s + l_s)/2} |0, 0\rangle$$

$$\text{where} \quad |0, 0\rangle = \sqrt{\omega_s/\pi \hbar} e^{-\omega_s(X_s^2 + Y_s^2)/2\hbar}$$

$$[18b] \quad C_{v_s, l_s} = \left\{ (2\omega_s \hbar)^{v_s} [(v_s + l_s)/2]! [(v_s - l_s)/2]! \right\}^{-\frac{1}{2}}$$

$$[18c] \quad l_s = \pm v_s, \pm(v_s - 2), \dots, \pm 1 \text{ or } 0$$

For this choice of functions and operators, we have the following results.

$$[19a] \quad \bar{H}_s |v_s, l_s\rangle = (v_s + 1) \hbar \omega_s |v_s, l_s\rangle$$

$$[19b] \quad \bar{H}_s = \bar{R}_{s+}^\dagger \bar{R}_{s+} + \omega_s (\bar{L}_{Z_s} + \hbar)$$

As a result of the commutation of \bar{H}_s and \bar{L}_{Z_s} , i.e. $[\bar{H}_s, \bar{L}_{Z_s}] = 0$, we also have the following result

$$[20] \quad \bar{L}_{Z_s} |v_s, l_s\rangle = l_s \hbar |v_s, l_s\rangle$$

For the operators \bar{P}_s^\pm and \bar{Z}_s^\pm we obtain the following results.

$$[21a] \quad \bar{Z}_s^\pm |v_s, l_s\rangle = (\pm i / \sqrt{2} \omega_s) [(v_s \pm l_s + 2) \hbar \omega_s |v_s + 1, l_s \pm 1\rangle - (v_s \mp l_s) \hbar \omega_s |v_s - 1, l_s \pm 1\rangle]$$

$$[21b] \quad \bar{P}_s^\pm |v_s, l_s\rangle = (\pm 1 / \sqrt{2}) [(v_s \pm l_s + 2) \hbar \omega_s |v_s + 1, l_s \pm 1\rangle + (v_s \mp l_s) \hbar \omega_s |v_s - 1, l_s \pm 1\rangle]$$

To complete the discussion of vibrational functions it is necessary to detail their transformation properties under the symmetry operations of the point groups concerned. In the case of the non-degenerate modes we are concerned with one dimensional representations and a detailed discussion would be superfluous.

In the case of the doubly degenerate modes two fold representations are involved, requiring a precise definition of how one's co-ordinates are chosen to transform.

We shall refer to $G_N \equiv C_N$ or S_N as the "Main generating Element" of the point group. The co-ordinates (X_{s_t}, Y_{s_t}) are a pair of normal co-ordinates corresponding to the s_t^{th} normal mode which span the degenerate species E_t . This pair of co-ordinates is defined to transform in the following manner under G_N .

$$[22] \quad G_N [\bar{Z}_{s_t}^+, \bar{Z}_{s_t}^-]^* \rightarrow [\bar{Z}_{s_t}^+, \bar{Z}_{s_t}^-] \begin{bmatrix} e^{-it\theta} & 0 \\ 0 & e^{it\theta} \end{bmatrix} \quad \theta = 2\pi/N$$

and it may also be shown that $(\bar{P}_{s_t}^+, \bar{P}_{s_t}^-)$ transform in the identical manner. Then from the previously given relations between

$\bar{Z}_{s_t}^\pm$ and $\bar{R}_{s_t}^\pm$ we see that $\bar{R}_{s_t}^\pm$ also transforms in this

fashion. That is, $G_N \bar{R}_{s_t}^\pm \rightarrow e^{\mp it\theta} \bar{R}_{s_t}^\pm$ from which we obtain immediately

$$[23] \quad G_N |v_{s_t}, l_{s_t}\rangle \rightarrow e^{-il_{s_t}\theta} |v_{s_t}, l_{s_t}\rangle$$

for the degenerate mode of species E_t .

* Note: (X_{s_t}, Y_{s_t}) actually transform into linear combinations of one another, but \bar{Z}_{s_t} was defined so that the effect of G_N would involve only the multiplication of the latter by an exponential phase factor.

$$(e \quad G_N [X_{s_t}, Y_{s_t}] \Rightarrow [X_{s_t}, Y_{s_t}] \begin{bmatrix} \cos \theta t & -\sin \theta t \\ \sin \theta t & \cos \theta t \end{bmatrix}$$

To complete the transformation details, it remains to specify the effects of two fold axes of rotation and reflection planes. This result is given in the equation below.

$$[24] \quad g_2 [\bar{X}_{s_t} \pm i \bar{Y}_{s_t}] \rightarrow [\bar{X}_{s_t} \mp i \bar{Y}_{s_t}]$$

where we use $g_2 = C_v \equiv C_{2a}$ for all groups except C_{Nv} in which case, due to absence of C_2 axes, we use $g_2 = \sigma_v \equiv \sigma(ac)$ as the defining operation. The adoption of these conventions determines the orientation of $[X_{s_t}, Y_{s_t}]$ in the a,b plane. Also, if we further require the characters of non-degenerate A and B types to be +1 or -1 according as 1 or 2 subscripts are involved, we uniquely determine the labels of these non-degenerate types*.

* As listed in Wilson, Decius and Cross for example.

(II-4) The Hamiltonian

Expanding the Hamiltonian we may write

$$[25a] \quad \bar{H} = \bar{H}_{ROT}^0 + \bar{H}_{VIB}^0 + \bar{H}_{V,R}^0 + \bar{H}_{V,R}^1$$

where

$$[25b] \quad \bar{H}_{ROT}^0 = (\bar{J}^2 - \bar{J}_c^2)/2I_b + \bar{J}_c^2/2I_c$$

$$[25c] \quad \bar{H}_{VIB}^0 = (1/2)[\sum_r(\bar{P}_r^2 + \omega_r^2 \bar{Q}_r^2) + \sum_s(\bar{P}_{X_s}^2 + \bar{P}_{Y_s}^2 + \omega_s(\bar{X}_s^2 + \bar{Y}_s^2))]$$

$$[25d] \quad \bar{H}_{V,R}^0 = -\bar{J}_c \bar{\Omega}_c / I_c$$

$$[25e] \quad \bar{H}_{V,R}^1 = -(\bar{J}_+ \bar{\Omega}_- + \bar{J}_- \bar{\Omega}_+)/2I_b$$

$$\bar{\Omega}_{\pm} = \bar{\Omega}_a \pm i\bar{\Omega}_b$$

As previously stated the $\bar{\Omega}_\alpha$ ($\alpha = a, b, c$) represent vibrational (internal) angular momentum, given by

$$[26] \quad \bar{\Omega}_\alpha = -\sum_{k,l} \zeta_{k,l}^\alpha \bar{Q}_l \bar{P}_k \quad \alpha = a, b, c$$

where k, l run over all normal co-ordinates. The constant ζ is called a coriolis coupling constant and is of primary importance in this study. It is related to the orthogonal transformation from the mass-weighted cartesian displacement co-ordinates, $q_{\alpha i}$, to normal co-ordinates, Q_k . The actual relation is as follows.

$$[27] \quad \zeta_{k,1}^c = \sum_i \delta(\bar{q}_k, \bar{q}_1) / \delta(\bar{q}_{ai}, \bar{q}_{bi})$$

-abc taken in cyclic order
-i sums over all atoms in molecule

$$\text{where } \delta(\bar{q}_k, \bar{q}_1) / \delta(\bar{q}_{ai}, \bar{q}_{bi}) = \begin{vmatrix} \delta\bar{q}_k / \delta\bar{q}_{ai} & \delta\bar{q}_k / \delta\bar{q}_{bi} \\ \delta\bar{q}_1 / \delta\bar{q}_{ai} & \delta\bar{q}_1 / \delta\bar{q}_{bi} \end{vmatrix}$$

from which it is readily seen that

$$\zeta_{k,1}^a = -\zeta_{1,k}^a \quad \text{and} \quad \zeta_{1,1}^a = 0$$

Each Ω_α contains the four distinct types of terms given below

$$[28] \quad (i) \quad \zeta_{X_s, Y_s}^a (\bar{X}_s \bar{P}_{Y_s} - \bar{Y}_s \bar{P}_{X_s}) = \zeta_{X_s, Y_s}^a \bar{L}_{Z_s}$$

$$(ii) \quad \zeta_{r, r'}^a (\bar{Q}_r \bar{P}_{r'} - \bar{Q}_{r'} \bar{P}_r)$$

$$(iii) \quad \zeta_{X_s, Y_s}^a (\bar{X}_s \bar{P}_{Y_s} - \bar{Y}_s \bar{P}_{X_s})$$

$$(iv) \quad \zeta_{r, X_s}^a (\bar{Q}_r \bar{P}_{X_s} - \bar{X}_s \bar{P}_r)$$

$$(v) \quad \zeta_{r, Y_s}^a (\bar{Q}_r \bar{P}_{Y_s} - \bar{Y}_s \bar{P}_r)$$

The effect of each of the different types of terms is outlined below in point form.

Type (i) Couple the two components of a degenerate mode.

Type (ii) Couple two non-degenerate modes.

Type (iii) Couple one component of a degenerate mode to one component of another degenerate mode.

Figure 1. (a) 1000 Hz, (b) 2000 Hz, (c) 3000 Hz, (d) 4000 Hz, (e) 5000 Hz, (f) 6000 Hz, (g) 7000 Hz, (h) 8000 Hz, (i) 9000 Hz, (j) 10000 Hz.



Figure 1. Frequency response of the system at different frequencies.

Figure 2. (a) 1000 Hz, (b) 2000 Hz, (c) 3000 Hz, (d) 4000 Hz, (e) 5000 Hz, (f) 6000 Hz, (g) 7000 Hz, (h) 8000 Hz, (i) 9000 Hz, (j) 10000 Hz.

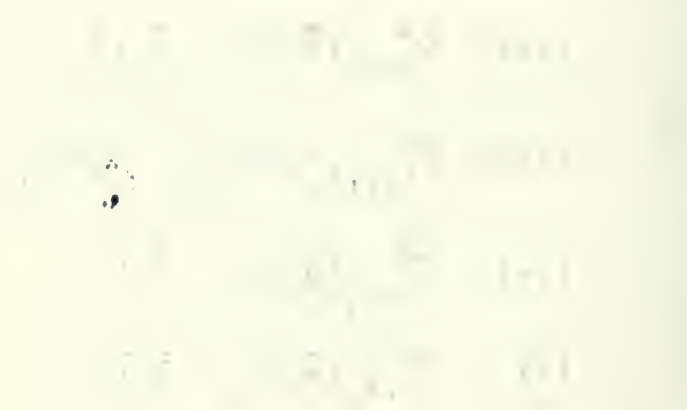


Figure 2. Frequency response of the system at different frequencies.

Figure 3. (a) 1000 Hz, (b) 2000 Hz, (c) 3000 Hz, (d) 4000 Hz, (e) 5000 Hz, (f) 6000 Hz, (g) 7000 Hz, (h) 8000 Hz, (i) 9000 Hz, (j) 10000 Hz.



Types (iv) and (v) Couple a non-degenerate mode to one component of a degenerate mode.

The molecular interactions considered will determine which terms may be neglected, in any given application. That is, one only considers those terms for which a measurable effect is expected. Clearly, for degenerate modes type (i) terms are always to be considered; this is simply the first order Coriolis effect that is typically seen in perpendicular absorption bands.

Using the relation [26] for Ω_α , symmetry operations may be applied to both sides of this equation. By comparing like terms on both sides of the transformed equation, one may obtain restrictions on the $\zeta_{k,1}^\alpha$ constants, based purely on symmetry arguments. The results tabulated below pertain to C_{N_V} and D_N type point groups where coupling between A_1 or A_2 to E type modes is considered.

Table I
Restrictions on $\zeta_{k,1}^\alpha$

$A_1(D_N)$ and $A_2(C_{N_V})$	$A_2(D_N)$ and $A_1(C_{N_V})$
$\zeta_{r,X_s}^c = \zeta_{r,Y_s}^c = 0$	$\zeta_{r,X_s}^c = \zeta_{r,Y_s}^c = 0$
$A \leftrightarrow E \quad \zeta_{r,Y_s}^a = \zeta_{r,X_s}^b = 0$	$\zeta_{r,X_s}^a = \zeta_{r,Y_s}^b = 0$
$\zeta_{r,X_s}^a = \zeta_{r,Y_s}^b$	$\zeta_{r,Y_s}^a = -\zeta_{r,X_s}^b$

By this means (symmetry restrictions) many terms in $\bar{\Omega}_\alpha$ may be omitted or combined with others to obtain a much simpler expression.

For coupling a non-degenerate mode with a degenerate component it is required to retain terms of types (i) and (iv) in the expansion of Ω_α . Thus we have the following results

$$[29a] \quad \bar{\Omega}_a = \sum_{r,s} [\zeta_{r,Y_s}^a (\bar{Q}_r \bar{P}_{Y_s} - \bar{Y}_s \bar{P}_r) + \zeta_{r,X_s}^a (\bar{Q}_r \bar{P}_{X_s} - \bar{X}_s \bar{P}_r)]$$

$$[29b] \quad \bar{\Omega}_b = \sum_{r,s} [\zeta_{r,Y_s}^b (\bar{Q}_r \bar{P}_{Y_s} - \bar{Y}_s \bar{P}_r) + \zeta_{r,X_s}^b (\bar{Q}_r \bar{P}_{X_s} - \bar{X}_s \bar{P}_r)]$$

$$[29c] \quad \bar{\Omega}_c = \sum_s [\zeta_{X_s,Y_s}^c (\bar{X}_s \bar{P}_{Y_s} - \bar{Y}_s \bar{P}_{X_s}) \equiv \zeta_{X_s,Y_s}^c \bar{L}_{Z_s}]$$

$$[29d] \quad \bar{\Omega}_\pm = \bar{\Omega}_a \pm i\bar{\Omega}_b = \sum_{r,s} [(\zeta_{r,X_s}^a \mp i\zeta_{r,Y_s}^a)(\bar{Q}_r \bar{P}_s - \bar{P}_r \bar{Z}_s)]$$

These results are general for A_1 and A_2 to E interactions for both C_{N_v} and D_N symmetries. For specific cases, the above expressions may be simplified further by reference to the preceeding table.

For our choice of basis set we note that

$$\begin{aligned} [30] \quad \bar{\Omega}_c \Pi_r |v_r\rangle \Pi_s |v_s, \lambda_s\rangle &= \Pi_r |v_r\rangle \bar{\Omega}_c \Pi_s |v_s, \lambda_s\rangle \\ &= \kappa(\sum_s \zeta_{X_s,Y_s}^c \lambda_s) \Pi_r |v_r\rangle \Pi_s |v_s, \lambda_s\rangle \end{aligned}$$

from which it readily follows that

$$\begin{aligned}
 [31] \quad \bar{H}_{VR}^0 \Psi_{VR} &= -(1/I_c) \bar{J}_c |J, \bar{M}\rangle \Pi_r |v_r\rangle \bar{\Omega}_c \Pi_s |v_s, l_s\rangle \\
 &= (-\hbar^2/I_c) k (\sum_s l_s \zeta_{X_s, Y_s}^c) \Psi_{VR}
 \end{aligned}$$

This is the first order Coriolis effect present in all degenerate modes of axially symmetric molecules.

It is now seen that the terms in \bar{H} with a "o" superscript give a diagonal contribution. Thus we could write $\bar{H} = \bar{H}^0 + \bar{H}^1$ where $\bar{H}^0 = \bar{H}_{ROT}^0 + \bar{H}_{VIB}^0 + \bar{H}_{VR}^0$ and $\bar{H}^1 = (\bar{J}_+ \hat{\Omega}_- + \bar{J}_- \hat{\Omega}_+)/2I_b$

It is this latter term \bar{H}^1 which results in what is commonly referred to as X-Y Coriolis coupling. The terms $\bar{\Omega}_c^2/2I_c$

and $(\bar{\Omega}_a^2 + \bar{\Omega}_b^2)/2I_b$ have been neglected, for reasons more readily understood after their effect has been explained.

We shall consider molecules in which there is a non-degenerate mode "r" of species A_1 or A_2 , nearly degenerate with a doubly degenerate mode "s" of species E_t . These two modes are in fact the only ones we shall account for; all others are assumed to be in a totally symmetric ground state supplying a constant (ignorable) energy. Further only single excitations, i.e. $v_r = 1, v_s = 0$ or $v_r = 0, v_s = 1$ (fundamentals), of these modes are considered. This means that we may reduce the product wavefunction

$\Pi_r |v_r\rangle \Pi_s |v_s, l_s\rangle$ to $|v_r\rangle |v_s, l_s\rangle$ and consider

interactions only between the following functions,

$$[32] \quad \begin{array}{ll} \text{(i)} & |1\rangle |0,0\rangle \\ \text{(ii)} & |0\rangle |1,+1\rangle \\ \text{(iii)} & |0\rangle |1,-1\rangle \end{array} \left. \vphantom{\begin{array}{l} \text{(i)} \\ \text{(ii)} \\ \text{(iii)} \end{array}} \right\} |0\rangle |1,\pm 1\rangle$$

where (i) is the non-degenerate fundamental and (ii) and (iii) the two components of the degenerate fundamental.

The effect of the neglected terms $(\bar{\Omega}_a^2 + \bar{\Omega}_b^2)/2I_b$ and $\bar{\Omega}_c^2/2I_c$ will now be detailed. The term $(\bar{\Omega}_a^2 + \bar{\Omega}_b^2)/2I_b$ may be written in terms of $\bar{\Omega}_\pm$ as below.

$$[33] \quad (\bar{\Omega}_a^2 + \bar{\Omega}_b^2)/2I_b = 1/4 I_b (\bar{\Omega}_+ \bar{\Omega}_- + \bar{\Omega}_- \bar{\Omega}_+)$$

The $\bar{\Omega}_\pm$ can be expressed in terms of \bar{R}_r^\pm , \bar{Z}_s^\pm and \bar{P}_s^\pm for which the effect on the $|v_r\rangle |v_s, l_s\rangle$ functions is known. Using this it may be found that this term creates matrix elements between $|v_r\rangle |v_s, l_s\rangle$ and the following functions.

$$[34] \quad \begin{array}{ll} \text{(i)} & |v_r\rangle |v_s, l_s\rangle \quad \text{Diagonal} \\ \text{(ii)} & |v_r^{\pm 2}\rangle |v_s, l_s\rangle \\ \text{(iii)} & |v_r\rangle |v_s^{\pm 2}, l_s\rangle \quad \text{Overtones} \\ \text{(iv)} & \left. \begin{array}{l} |v_r^{\pm 2}\rangle |v_s^{\pm 2}, l_s\rangle \\ |v_r^{\pm 2}\rangle |v_s^{\mp 2}, l_s\rangle \end{array} \right\} \quad \text{Combinations} \end{array}$$

Type (i) terms are the only terms of possible interest here since the combinations and overtones will be well removed from the degeneracy considered. The approximate value of the matrix element obtained for term (i) is given below, for $A_1 \leftrightarrow E$ of C_{N_v}

$$[35a] \quad 1/4 I_b \langle 0 | \langle 1, \pm 1 | (\bar{\Omega}_+ \bar{\Omega}_- + \bar{\Omega}_- \bar{\Omega}_+) | 0 \rangle | 1, \pm 1 \rangle$$

$$\doteq -2.5 B_{\perp} (\zeta_{r, Y_s}^a)^2 (\text{cm}^{-1})$$

$$[35b] \quad 1/4 I_b \langle 1 | \langle 0, 0 | (\bar{\Omega}_+ \bar{\Omega}_- + \bar{\Omega}_- \bar{\Omega}_+) | 1 \rangle | 0, 0 \rangle$$

$$\doteq -2.8 B_{\parallel} (\zeta_{r, Y_s}^a)^2 (\text{cm}^{-1})$$

Thus $(\bar{\Omega}_a^2 + \bar{\Omega}_b^2)/(2I_b)$ has the effect of shifting the entire

degenerate and non-degenerate bands in the same direction by slightly differing amounts. This effect is not felt of real significance and has been neglected. The term $\bar{\Omega}_c^2/2I_c$ will have the following effect for the terms retained in $\bar{\Omega}_c$

$$\begin{aligned} [36] \quad & \langle v_r | \langle v_s, l_s | \bar{\Omega}_c^2/2I_c | v_r \rangle | v_s, l_s \rangle \\ &= A (\zeta_{X_s, Y_s}^c l_s)^2 (\text{cm}^{-1})^* \\ &= 0 \quad \text{if} \quad v_s = 0 \end{aligned}$$

* This term corresponds to the term $\sum_i \sum_{k \neq i} g_{ik} l_i l_k$ in the vibrational energy formula given in Herzberg, vol. II, pp. 210.

This again represents a small shift in the degenerate band-origin and shall be ignored.

It remains to determine the non-diagonal matrix elements arising from \bar{H}^1 . We first note that levels corresponding to $|J,K\rangle$ and $|J,-K\rangle$, $K = |k|$, are degenerate (usual k degeneracy) and define the following new functions.

$$[37a] \quad |+\ell, K, p\rangle = \sqrt{1/2} \left\{ |0, 1^{+1}; J, K\rangle + p |0, 1^{-1}; J, -K\rangle \right\} \quad K \geq 0, p = \pm$$

$$[37b] \quad |-\ell, K, p\rangle = \sqrt{1/2} \left\{ |0, 1^{-1}; J, K\rangle + p |0, 1^{+1}; J, -K\rangle \right\} \quad K > 0, p = \pm$$

$$[37c] \quad |K, p\rangle = \sqrt{1/2} \left\{ |1, 0; J, K\rangle + p |1, 0; J, -K\rangle \right\} \quad K > 0, p = \pm$$

$$[37d] \quad |0, p\rangle = |1, 0; J, 0\rangle \quad K = 0, p = \pm \text{ only}$$

$$\text{where } |v_r, v_s^{\ell_s}; J, K\rangle = |v_r\rangle |v_s^{\ell_s}\rangle |JK\rangle$$

Note that we will refer to the $K=0$ function in [37a]

as $|-\ell, 0, p\rangle$ rather than as $|+\ell, 0, p\rangle$ (see for example Table II).

The above results apply for $A_1 \leftrightarrow E$ coupling and $A_2 \leftrightarrow E$ coupling in C_{N_v} and D_N symmetry types, respectively. For $A_2 \leftrightarrow E$ and $A_1 \leftrightarrow E$ coupling in C_{N_v} and D_N symmetries respectively, the last two functions should be multiplied by $(-i)$ so that real and positive matrix elements result.

It is in terms of these new functions that we obtain the following energy matrices for the complete Hamiltonian, $\bar{H} = \bar{H}^0 + \bar{H}^1$, where off diagonal terms are due to \bar{H}^1 :

Table II
Energy Matrix for $K > 0$
 $[A_1 - E(C_{Nv}) \text{ and } A_2 - E(D_N)]^*$

$K > 0; p = \pm$	$\langle -1, K-1, p $	$\langle K, -p $	$\langle +1, K+1, p $
$ -1, K-1, p \rangle$	$B_L J(J+1) + (A_L - B_L)(K-1)^2$ $+ 2A_L \zeta_{X_s Y_s}^C (K-1) + \nu_s$	$B' \zeta_{r, Y_s}^a \sqrt{(J+K)(J-K+1)}$ $x p \text{ for } K=1$	0
$ K, -p \rangle$	$B' \zeta_{r, Y_s}^a \sqrt{(J+K)(J-K+1)}$ $x p \text{ for } K=1$	$B_{ } J(J+1) + (A_{ } - B_{ })K^2$ $+ \nu_r$	$-B' \zeta_{r, Y_s}^a \sqrt{(J-K)(J+K+1)}$
$ +1, K+1, p \rangle$	0	$-B' \zeta_{r, Y_s}^a \sqrt{(J-K)(J+K+1)}$	$B_{\perp} J(J+1) + (A_{\perp} - B_{\perp})(K+1)^2$ $- 2A_L \zeta_{X_s Y_s}^C (K+1) + \nu_s$

$-B_L, A_L$ are rotational constants pertaining to the degenerate mode.
 $-B_{||}, A_{||}$ are rotational constants pertaining to the non degenerate mode.
 $-B' = (1/2\sqrt{2})(B_L + B_{||})(\sqrt{\nu_r/\nu_s} + \sqrt{\nu_s/\nu_r})$

* Only these cases are considered in detail.

Table III
Energy Matrix for $K = 0$
 $[A_1 - E(C_{NV}) \text{ and } A_2 - E(D_N)]$

$K = 0$	$\langle 0, + $	$\langle +1, 1, - $	$\langle +1, 1, + $
$ 0, + \rangle$	$B_{ }J(J+1) + \nu_r$	$-B' \zeta_{r, Y_s}^a \sqrt{2J(J+1)}$	0
$ +1, 1, - \rangle$	$-B' \zeta_{r, Y_s}^a \sqrt{2J(J+1)}$	$B_{\perp}J(J+1) + (A_{\perp} - B_{\perp}) - 2A_{\perp} \zeta_{X_s, Y_s + \nu_s}^c$	0
$ +1, 1, + \rangle$	0	0	$B_{\perp}J(J+1) + (A_{\perp} - B_{\perp}) - 2A_{\perp} \zeta_{X_s, Y_s + \nu_s}^c$

Note that the two matrices for $K = 1$ are different, since p multiplies the indicated off-diagonal matrix elements. However, the same results for intensities and energies are obtained if we ignore this exception.

For clarity in the following discussion, note that K' will refer to the $|K|$ value of the non-degenerate mode in the energy matrix. Thus $0 \leq K' \leq J'+1$.

It may be noted that for the basis set making up the eigenvectors that $J \geq K$ and for $K = 0$ we define the special function $|0, +\rangle$. Thus $K' = 0$ is a special case for which the 3×3 reduces to a 1×1 or a 2×2 , according as the $p \equiv +$ or $p \equiv -$ combinations are considered. As a result the $p \equiv +$ and $p \equiv -$ combination matrices for $K' = 0$ must be independently created and diagonalized. It is clear that the 1×1 result requires no diagonalization and represents a state that is unperturbed by this interaction.

Chapter III

INFRARED AND RAMAN INTENSITY THEORY(III-1) Introduction

To facilitate the calculation of the transition moments (matrix elements) we shall define the following functions.

$$[37'] |A, E; J', K', p'\rangle = a_- |-\ell, K'-1, p'\rangle + a_0 |K', -p'\rangle + a_+ |+\ell, K'+1, p'\rangle$$

where $|A, E; J', K', p'\rangle$ is the upper (final) state eigenvector

and $|J, K, p\rangle$ the lower (initial) state assumed to be in its

totally symmetric vibrational ground state. The coefficients a_- , a_0 , a_+ are obtained along with corresponding eigenvalues from the diagonalization of the previously described energy matrix for J' and K' where $0 \leq K' \leq J' + 1$

For the integrals $\langle A, E; J', K', p' | \bar{\mu} | J, K, p \rangle$ and

$\langle A, E; J', K', p' | \bar{\alpha} | J, K, p \rangle$ for infrared and Raman respectively, one may obtain frequencies and relative intensities. The frequency shifts are simply the difference between the final state eigenvalue and initial state rotational energy. The relative intensities for Raman and infrared transitions may be obtained from the following expression.

$$[38] \quad I = (\text{Frequency Factor}) (2J+1) g_{JK} \left| M_{J,K,0}^{J',K',1} \right|^2 e^{-E_0(J,K)/kT}$$

(Frequency Factor) = $\Delta\nu$ for infrared; $(\nu_e - \Delta\nu)^4$ for Raman.

Note - J' , K' are the rotational quantum numbers of the final

state eigenvector.

- J, K are the rotational quantum numbers of the initial state.
- $(2J+1)$ is a space fixed degeneracy factor from the space fixed M quantum number.
- g_{JK} is a nuclear spin degeneracy factor more usually referred to as the nuclear statistical weight. This number is calculated by the methods outlined in Landau and Lifshitz.
- $F_0(J,K)$ is the rotational energy of the initial state; it appears in the usual Boltzman factor for population of the lower state.
- $\Delta\nu$ is the difference in energy between the initial state and final state eigenvector.
- ν_E is the frequency of the exciting line in the case of Raman scattering.
- $M_{J,K,0}^{J',K',1}$ is the infrared or Raman transition moment as the case may be.

Since "Rigid Rotor" functions were used as an initial basis set, the

$M_{J,K,0}^{J',K',1}$ may be expressed in terms of the well known transition

moments of these functions. How these transition moments are obtained for both the infrared and Raman cases is given in following sections.

(III-2) Infrared Transition moments.

We evaluate $\langle A, E; J', K', p' | \bar{\mu} | J, K, p \rangle$, noting that only one component $\bar{\mu}_\alpha$ of the space fixed dipole moment operator $\bar{\mu}$ need be considered for random systems. By convention we choose to consider $\bar{\mu}_Z$, and find that $\bar{\mu}_Z$ is related to its molecule fixed counterparts as follows.

$$[39] \quad \bar{\mu}_Z = \bar{f}_{Za}(\theta, \phi, \chi) \bar{\mu}_a + \bar{f}_{Zb}(\theta, \phi, \chi) \bar{\mu}_b + \bar{f}_{Zc}(\theta, \phi, \chi) \bar{\mu}_c$$

Considering the molecule fixed spherical combinations $\bar{\mu}_0 = \bar{\mu}_c$ and $\bar{\mu}_{\pm 1} = (1/\sqrt{2})(\bar{\mu}_a \pm i\bar{\mu}_b)$ we write,

$$[40] \quad \bar{\mu}_Z = \sum_r \bar{F}_{-r} \bar{\mu}_r ; r = 0, \pm 1$$

where the \bar{F}_{-r} are appropriate linear combinations of the $\bar{f}_{Z\alpha}$ ($\alpha=a,b,c$). The $\bar{f}_{Z\alpha}$ contain a dependence on the magnetic quantum number m , via the ϕ in $\bar{f}_{Z\alpha}$. This m dependence when averaged over all m values, leads to well-known results for the individual basis functions

$$[41] \quad \langle \Psi' | \sum_r \bar{F}_{-r} \bar{\mu}_r | \Psi \rangle = \sum_r \langle \Psi' | \bar{\mu}_r | \Psi \rangle \langle J', K' | \bar{F}_{-r} | J, K \rangle$$

where \bar{F}_{-r} is referred to as a reduced operator whose matrix elements are conveniently presented in Table V of Lepard (1970). Using these results we collect all terms in $\langle A, E; J', K', p' | \bar{\mu} | J, K, p \rangle$ to obtain transition moments, following the next discussion on vibrational moments.

Vibrational moments.

The dipole moment may be expanded in a Taylor series of the normal co-ordinates about the equilibrium position

$$[42] \text{ ie } \bar{\mu}_{\alpha}(Q_1, \dots, Q_{3N-6}) = (\bar{\mu}_{\alpha})_e + \sum_{k=1}^{3N-6} (\delta \bar{\mu}_{\alpha} / \delta \bar{Q}_k)_e \bar{Q}_k +$$

$$\alpha = a, b, c$$

where the first term represents pure rotation, (i.e. no vibrational transition) not of interest in this application, and the second term only is retained.

That is,

$$[43] \quad \bar{\mu}_{\alpha} = \sum_{k=1}^{3N-6} (\delta \bar{\mu}_{\alpha} / \delta \bar{Q}_k)_e \bar{Q}_k$$

When we treat degenerate and non-degenerate co-ordinates independently the above equation becomes;

$$[44] \quad \bar{\mu}_{\alpha} = \sum_r (\delta \bar{\mu}_{\alpha} / \delta \bar{Q}_r)_e \bar{Q}_r + \sum_s ((\delta \bar{\mu}_{\alpha} / \delta \bar{X}_s)_e \bar{X}_s + (\delta \bar{\mu}_{\alpha} / \delta \bar{Y}_s)_e \bar{Y}_s)$$

r - runs over all non degenerate modes,

s - runs over all degenerate modes,

and Q_r, X_s, Y_s are the co-ordinates defined in the description of the vibrational functions, and transform as previously detailed.

Noting that $\bar{\mu}_{\alpha}$ transforms as \bar{T}_{α} we may apply symmetry considerations to obtain the following results

$$[45a] \quad \bar{\mu}_0 = \sum_r (\delta \bar{\mu}_0 / \delta \bar{Q}_r)_e \bar{Q}_r \quad \text{where } Q_r \text{ is of type } A_1(C_{Nv}) \text{ or } A_2(D_N)$$

$$[45b] \quad \bar{\mu}_{\pm 1} = 1/\sqrt{2} \sum_s (\delta \bar{\mu}_{\alpha} / \delta \bar{X}_s)_e \bar{X}_{s\pm}$$

$\therefore \quad \frac{1}{\sqrt{2}} = \sin A$

Since we consider only one degenerate and one non degenerate mode labelled r and s, respectively, we reduce the above to the following

$$[46a] \quad \bar{\mu}_0 = (\delta\bar{\mu}_c/\delta\bar{Q}_r)_e \bar{Q}_r$$

$$[46b] \quad \bar{\mu}_{\pm 1} = (1/\sqrt{2})(\delta\bar{\mu}_a/\delta\bar{X}_s)_e \bar{Z}_{s\pm}$$

Note that both \bar{Q}_r and $\bar{Z}_{s\pm}$ give rise to purely imaginary matrix elements.

The vibrational functions that we shall consider in the final state are $\langle 0 | \langle 1, \pm 1 |$ and $\langle 1 | \langle 0, 0 |$, and all non-zero vibrational transition matrix elements between these and the initial state $|0\rangle |0, 0\rangle$ are given in table IV below.

Table IV
Infrared Vibrational Matrix Elements

Final state $\bar{\mu}_r 0\rangle 0,0\rangle$	$\langle 0 \langle 1, \pm 1 $	$\langle 1 \langle 0, 0 $
$\bar{\mu}_{\pm 1} 0\rangle 0,0\rangle$	$\mu_{\pm} = -i\sqrt{\hbar/4\pi c v_s} (\delta\bar{\mu}_a/\delta\bar{X}_s)_e$	0
$\bar{\mu}_0 0\rangle 0,0\rangle$	0	$\mu_0 = -i\sqrt{\hbar/4\pi c v_r} (\delta\bar{\mu}_c/\delta\bar{Q}_r)_e$ Q of $A_1(C_{Nv})$ or $A_2(D_N)$ species

1. The first part of the paper is devoted to a study of the properties of the function $f(x)$ defined by the equation $f(x) = \int_0^x f(t) dt$. It is shown that $f(x)$ is a constant function.

2. In the second part, we consider the function $g(x)$ defined by the equation $g(x) = \int_0^x g(t) dt$. It is shown that $g(x)$ is a constant function.

1	The first part of the paper is devoted to a study of the properties of the function $f(x)$ defined by the equation $f(x) = \int_0^x f(t) dt$. It is shown that $f(x)$ is a constant function.
2	In the second part, we consider the function $g(x)$ defined by the equation $g(x) = \int_0^x g(t) dt$. It is shown that $g(x)$ is a constant function.
3	The third part of the paper is devoted to a study of the properties of the function $h(x)$ defined by the equation $h(x) = \int_0^x h(t) dt$. It is shown that $h(x)$ is a constant function.

Here ν_r and ν_s are in cm^{-1} . Note that the results for the matrix elements of \bar{Q}_r and \bar{Z}_{st} were previously given, and therefore $\mu_{||}$ and μ_{\perp} are completely determined by specifying values, from experimental spectra, for the derivatives

Using these results we obtain the transition matrix elements

$\langle A, E; J', K', p' | \bar{\mu} | J, K, p \rangle$ given in Table V.

As previously remarked, the intensity factors

in Table V have been previously tabulated by Lepard (1970). The transition matrix elements are tabulated for individual basis functions and hence one must sum these results tabulated for all allowed eigenvector basis functions. That is

$$[47] \quad M_{J,K,p}^{J',K',p'} = \{E(+1)\} + \{A_1 C_{3v} \text{ or } A_2 D_3\} + \{E(-1)\}$$

where $M_{J,K,0}^{J',K',1}$ is now the total transition moment.

It should also be noted that both $\mu_{||}$ and μ_{\perp} are purely imaginary, but since the intensity involves the modulus squared it is necessary only that moments be either all imaginary or all real.

Table V

$$\langle A, E; J', K', P' | \sum_{\mathbf{r}} \bar{f}_{-\mathbf{r}} \bar{\mu}_{\mathbf{r}} | J, K, P \rangle$$

Basis Function	$K > 0$	$K = 0; (P = + \text{ only})$	
		$P' \equiv +; (1 \times 1 \text{ matrix})$	$P' \equiv -; (2 \times 2 \text{ matrix})$
$E(-\chi)$	$a_- \mu_{\perp} \langle J', K-1 \bar{f}_+ J, K \rangle = I_-$ multiply by P' for $K=1$		
$A_1 C_{3v}$	$a_0 \mu_{\parallel} \langle J', K \bar{f}_0 J, K \rangle = I_{O_1}$		I_{O_1}
$A_2 D_3$	$a_0 \mu_{\parallel} \langle J', K \bar{f}_0 J, K \rangle = I_{O_2}$		I_{O_2}
$E(+\chi)$	$a_+ \mu_{\perp} \langle J', K+1 \bar{f}_- J, K \rangle = I_+$	$\sqrt{2} I_+$ $a_+ \equiv 1$	$\sqrt{2} I_+$
$\Delta J = 0 \text{ for } P' = P; \Delta J = \pm 1 \text{ for } P' = -P$			

(III-3) Raman Moments

It is necessary to evaluate $\langle A, E; J', K', P' | \bar{\alpha} | J, K, P \rangle$ where $\bar{\alpha}$ represents the space fixed polarizability tensor whose significance is displayed below, in terms of an induced dipole moment $\bar{\mu}_i$ and an electric field \vec{E} :

$$[48] \quad [\bar{\mu}_{iX}, \bar{\mu}_{iY}, \bar{\mu}_{iZ}] = [E_X, E_Y, E_Z] \begin{bmatrix} \alpha_{XX} & \alpha_{XY} & \alpha_{XZ} \\ \alpha_{YX} & \alpha_{YY} & \alpha_{YZ} \\ \alpha_{ZX} & \alpha_{ZY} & \alpha_{ZZ} \end{bmatrix}$$

That is, we evaluate "induced dipole" matrix elements.

The tensor $\bar{\alpha}$ may be written as a combination of trace, anti-symmetric and symmetric components of rank $R = 0, 1, 2$, respectively.

$$[49] \quad \text{ie } \bar{\alpha}_{ij} = \sum_{R=0,1,2} \sum_{r=0,\pm 1 \dots \pm R} (n_{ij})_r^R \bar{\alpha}_r^R; \quad ij = x, y \text{ or } z$$

where the n 's are numerical factors. Note that $R=0$ and 2 represent isotropic and anisotropic scattering respectively and that we primarily consider the latter. Analogous to the infrared case we consider spherical components of the space fixed dipole, related to the molecule fixed spherical components via the Euler angle transformation. As in the infrared case we obtain a dependence on the magnetic quantum number " m " which must be averaged. When this has been done we again

$$[50] \quad |\langle \Psi' | \bar{\alpha}_{ij} | \Psi \rangle|^2 = \sum_R (C_{ij}^R / (2R+1)) \left| \left(\sum_r \langle \Psi' | \bar{\alpha}_r^R | \Psi \rangle \langle J', K' | \bar{F}_{-r}^R | J, K \rangle \right)^2 \right. \\ \left. i, j = X, Y, Z \right.$$

where \bar{F}_{-r}^R is a reduced operator containing the averaged " m " dependence. The matrix elements of \bar{F}_{-r}^R are presented in convenient

* In this and all following such expressions the electric field is omitted.

form in Table VI (Lepard 1970). It is evident that intensity contributions for different ranks are additive. This is a result of the fact that when the averaging over "m" is performed, cross terms between different ranks vanish. It may also be thought of as a result of the orthogonality of the \bar{a}_r^R , $R = 0, 1$ and 2 , which are isomorphous to the spherical harmonics for $L = 0, 1$ and 2 .

Since Raman is a scattering effect, the direction and polarization of the incident and scattered radiation are of significance. That is, different intensities of the scattered radiation may be obtained by manipulating these parameters. The case that is considered herein corresponds to radiation polarized in the Z direction, incident in the X direction and the X polarization component of radiation scattered in the Y direction is viewed. For this case we obtain using Table III (Lepard 1970)

$$[51] \quad I_{\perp} = I_{ZX} = (\nu_e - \Delta\nu)^4 g_{JK} (2J+1) e^{-F_0/kT} \left(\frac{1}{10} G^{(2)} \right)$$

where I_{ZX} is the relative intensity and

$$G^{(R)}(R=0,1,2) = \left| \sum_r \langle \Psi_v' | \bar{a}_r^R | \Psi_v \rangle \langle J', K' | \bar{F}_{-r}^R | J, K \rangle \right|^2$$

As a result we need not consider isotropic (trace) scattering, $I_{\parallel} = I_{ZZ}$, although moments for these transitions will be separately presented.

Note that the intensity formula for the other polarization, I_{\parallel} , is as above except that $(1/10)G^{(2)}$ must be replaced by $G^{(0)}/3 + G^{(2)}/15$

Vibrational Moments

Analogous to infrared we write

$$[52] \quad \bar{a}_r^R = (\bar{a}_r^R)_e + \sum_{k=1}^{3N-6} (\partial \bar{a}_r^R / \partial \bar{q}_k)_e \bar{q}_k + \dots$$

and following identical procedures (i.e. grouping co-ordinates as degenerate and non-degenerate) and applying symmetry considerations we obtain the following results:

$$[53a] \quad \bar{a}_0^2 = \left\{ \sqrt{3/2} (\partial \bar{a}_{cc} / \partial \bar{q}_r)_e - \sqrt{1/6} (\partial \bar{T} / \partial \bar{q}_r)_e \right\} \bar{q}_r$$

where $\bar{T} = \bar{a}_{aa} + \bar{a}_{bb} + \bar{a}_{cc}$ is the Trace, and this term exists only if \bar{q}_r is of totally symmetric species,

$$[53b] \quad \bar{a}_{\pm 1}^2 = (\partial \bar{a}_{ac} / \partial \bar{x}_s)_e \bar{z}_{s\pm} \text{ for } C_{3v}$$

$$= \pm i (\partial \bar{a}_{ab} / \partial \bar{x}_s)_e \bar{z}_{s\pm} \text{ for } D_3,$$

$$[53c] \quad \bar{a}_{\pm 2}^2 = -(\partial \bar{a}_{ab} / \partial \bar{y}_s)_e \bar{z}_{s\mp} \text{ for } C_{3v} \text{ or } D_3.$$

$$[53d] \quad \text{Note also } \bar{a}_0^0 = (1/\sqrt{3}) (\partial \bar{T} / \partial \bar{q}_r)_e \bar{q}_r$$

for \bar{q}_r of totally symmetric species only.

Note that in the above expressions the \bar{a}_r^R are as defined by (Lepard 1970). All non-zero vibrational transition matrix elements are given in Table VI below.

Table VI

Raman Vibrational Matrix Elements

[Final state] $\bar{a}_{-r}^R \text{initial state} \rangle$	$\langle 1 \langle 1, \frac{1}{2} 1 $	$\langle 1 \langle 00 $
$\bar{a}_0^0 0 \rangle 00 \rangle$		$a_0^0 = (-i/\sqrt{3})(\partial \bar{T}/\partial \bar{Q}_r)_e \sqrt{\hbar/4\pi c \nu_r}$ for C_{3v} ; \bar{Q}_r of A_1 species only
$\bar{a}_0^2 0 \rangle 00 \rangle$		$a_0^2 = \left\{ \begin{array}{l} \sqrt{3/2}(\partial \bar{a}_{cc}^0/\partial \bar{Q}_r) \\ -1/\sqrt{6}(\partial \bar{T}/\partial \bar{Q}_r)_e \end{array} \right\} (-i\sqrt{\hbar/4\pi c \nu_r})$ for C_{3v} ; \bar{Q}_r of species A_1 only
$\bar{a}_1^2 0 \rangle 00 \rangle$	$a_1^2 = -i\sqrt{\hbar/2\pi c \nu_s}(\partial \bar{a}_{ac}^0/\partial \bar{X}_s)_e : C_{3v}$ $= \pm i\sqrt{\hbar/2\pi c \nu_s}(\partial \bar{a}_{bc}^0/\partial \bar{X}_s)_e : D_3$	
$\bar{a}_2^2 0 \rangle 00 \rangle$	$a_2^2 = +i\sqrt{\hbar/2\pi c \nu_s}(\partial \bar{a}_{ab}^0/\partial \bar{Y}_s)_e : C_{3v}$ or D_3	

Using the wavefunctions in eqs [37] the results in Table VI yield

$$\begin{aligned}
 [54] \quad a_- \left[\alpha_{-1}^2 \langle J', K'-1 | \bar{F}_{+1}^2 | J, K \rangle + \alpha_{+2}^2 \langle J', K'-1 | \bar{F}_{-2}^2 | J, K \rangle \right] \\
 + a_0 \left[\alpha_0^2 \langle J', K' | \bar{F}_0^2 | J, K \rangle \right] \\
 + a_+ \left[\alpha_{+1}^2 \langle J', K'+1 | \bar{F}_{-2}^2 | J, K \rangle + \alpha_{-2}^2 \langle J', K'+1 | \bar{F}_{+2}^2 | J, K \rangle \right]
 \end{aligned}$$

where the α 's are parameters that may be assigned values through a comparison of observed with calculated spectra, although in principle they may be calculated by evaluating the derivatives in Table VI; the various cases for K' , not necessarily equal to K , are given in Tables VII and VIII for $R=2$ and Table IX for $R=0$ (isotropic scattering).

These tables contain all non-zero transition matrix elements for both the symmetric component and trace of the scattering tensor. The matrix elements are given for individual basis functions, and hence one must sum the matrix elements given for all the allowed eigenvector basis functions. That is

$$[55] \quad M_{J, K, 0}^{J', K', 1} = \left\{ E(+l) \right\} + \left\{ A_1(C_{3v}) \text{ or } A_2(D_3) \right\} + \left\{ E(-l) \right\}$$

where $M_{J, K, 0}^{J', K', 1}$ is the total transition moment.

Table VII

$$\langle A, E; J', K', P' | \sum_r \bar{F}_r^{-2} \bar{a}_r^{-2} | J, K, P \rangle$$

$\Delta K = 0$			
Basis Function		$K = 0 ; (P = + \text{ only})$	
		$P' = + ; (1 \times 1 \text{ matrix})$	$P' = - ; (2 \times 2 \text{ matrix})$
$E(-)$	$\gamma a_- \alpha_{+1}^2 \langle J', K-1 \bar{F}_{+1}^{-2} J, K \rangle = I$ multiply by P' for $K=1$		
$A_1(C_{3v})$	$a_0 \alpha_0^2 \langle J', K \bar{F}_0^{-2} J, K \rangle = I_0$		I_0
$E(+)$	$a_+ \alpha_{+1}^2 \langle J', K \bar{F}_{-1}^{-2} J, K \rangle = I_+$	$\sqrt{2} I_+ ; a_+ \equiv 1$	$\sqrt{2} I_+$
$\Delta J = 0, \pm 2 \text{ for } P' \equiv -\eta P ; \Delta J = \pm 1 \text{ for } P' \equiv +\eta P : \eta = \begin{Bmatrix} + C_{3v} \\ - D_3 \end{Bmatrix}$			

Table VIIIa

 $\langle A, E; J'K', p' | \sum_{\mathbf{r}} \bar{F}_{-\mathbf{r}}^2 \bar{\alpha}_{\mathbf{r}}^2 | J, K, p \rangle$

Basis Function	$\Delta K = +3$		$\Delta K = -3$ $K > 2$
	$K > 0$	$K = 0; p \equiv + \text{ only}$	
$E(-1)$	$a_- \alpha_{+2}^2 \langle J', K+2 \bar{F}_{-2}^2 J, K \rangle$ $= I_-$	$\sqrt{2} I_-$	
$A_1(C_{3v})$			
$E(+1)$			$a_+ \alpha_{+2}^2 \langle J', K-2 \bar{F}_{+2}^2 J, K \rangle$ $(a_+ \equiv 1 \text{ for } K=3, p' \equiv +)$
$\Delta J = 0, \pm 2 \text{ for } p'=p \quad \Delta J = \pm 1 \text{ for } p'=-p$			

Table VIIIb

 $\langle A, E; J', K', p' | \sum_{\mathbf{r}} \bar{F}_{-\mathbf{r}}^2 \bar{\alpha}_{\mathbf{r}}^2 | J, K, p \rangle$

Basis Function	$\Delta K = -1; K = 2 \text{ only}$		$\Delta J = \pm 1 \text{ for } p'=-p$
	$\Delta K = +1; K = 1 \text{ only}$	$a_- \alpha_2^2 \langle J', 0 \bar{F}_{+2}^2 J, K \rangle$	
$E(-1)$	$a_{-p'} \alpha_2^2 \langle J', -1 \bar{F}_{+2}^2 J, 1 \rangle$		
$\Delta J = 0, \pm 2 \text{ for } p'=p$			

Table IX
 $\langle A_j E J J', K', P' | \bar{F}_0^0 \bar{\alpha}_0^0 | J, K, P \rangle$

Basis Function	$K > 0$	$K = 0 \quad P \equiv + \text{ only}$	
		$P' \equiv +$	$P' \equiv -$
$A_1 (C_{3v})$	$a_0 \alpha_0^0 \langle JK \bar{F}_0^0 JK \rangle$	—	$a_0 \alpha_0^0 \langle J, K \bar{F}_0^0 JK \rangle$

Chapter IV

COMPUTATIONAL DETAILS

(IV-1) Introduction

The computations in this work are involved with the generation of simulated molecular spectra which may be confidently compared with their experimental counterparts. Due to the large number of transitions that must be calculated this is most easily done using a digital computer.

An algorithm was written to compute these simulated spectra. The two main functions of this algorithm are detailed below.

- (i) A table of relative intensity is created and stored internally in the computer as an array.
- (ii) Once the intensity table has been created it is transformed in such a way as to supply a final spectra to be compared with experiment. It is this portion of the algorithm which is most critical if meaningful results are to be obtained. This section of the algorithm is composed of the following subsections.
 - (a) Line Broadening.
 - (b) Conversion to Absorption (Infrared).
 - (c) Slit convolution.
 - (d) Photographic or Photoelectric response.

Each component of the algorithm will now be presented in greater detail so that their purpose and significance will be clarified.

(IV-2) Algorithm Details.

(i) Line intensity Table:

This table is generated by sequentially choosing each possible J' , K' pair of the non-degenerate component of the final state. For each J' , K' pair the final state energy matrix is created and diagonalized, then all (Raman or infrared) transitions involving this final state eigenvector are obtained for all allowed initial states. For each such transition a frequency and relative intensity are calculated using previously given formulae. These relative intensities are accumulated into segments of a linear array according to their frequency. This process continues until the Boltzman factor becomes so small that any remaining transitions would have no noticeable cumulative effect on the computed spectrum.

The relative intensity table that has been calculated is a line spectrum. Each theoretical intensity, like their Euclidean counterparts, have length but no breadth. In practice each line is spread over some "statistical" frequency distribution. This effect, often referred to as line broadening (discussed by Michelson (1895) and later in greater detail by Breene (1964)) is assumed to have at least four causes.

- (i) Radiation damping (natural line breadth).
- (ii) Doppler Effect.
- (iii) Resonance between near molecules.
- (iv) Pressure broadening.

In the present application pressure broadening is the dominant effect, but for the low pressures concerned it was decided unnecessary to include this effect. This choice was primarily a result of the fact that we calculate frequencies to 0.05 cm^{-1} intervals, and the half width of pressure broadening is probably less than this.

Conversion to Absorption (Infrared)

In the case of infrared spectra it is usually necessary to convert one's relative intensities to absorption. This is done in our case by applying the following transformation to the contents of every array segment.

$$[56] \quad A_i = 100(1 - \exp(-S_i \times N))$$

- S_i is the accumulated theoretical intensity in the i^{th} array segment.

- N is a scale factor chosen so that when the final spectra is output one of the computed peaks matches the absorption of its experimental counterpart.

- A_i is the calculated absorption which replaces S_i in the i^{th} array segment.

Slit Convolution or Broadening.

To properly handle this problem, one must determine the type of experimental detection concerned so that one may choose a proper slit convolution.

In our case the infrared spectra were obtained using a

Perkin Elmer #225 grating infrared spectra photometer. For this apparatus a Gaussian slit convolution was felt justifiable. The width at half height of this Gaussian is equal to the "spectral slit width" of the exit slit.

The diagram below depicts the relation between the "spectral slit width" and the Gaussian.

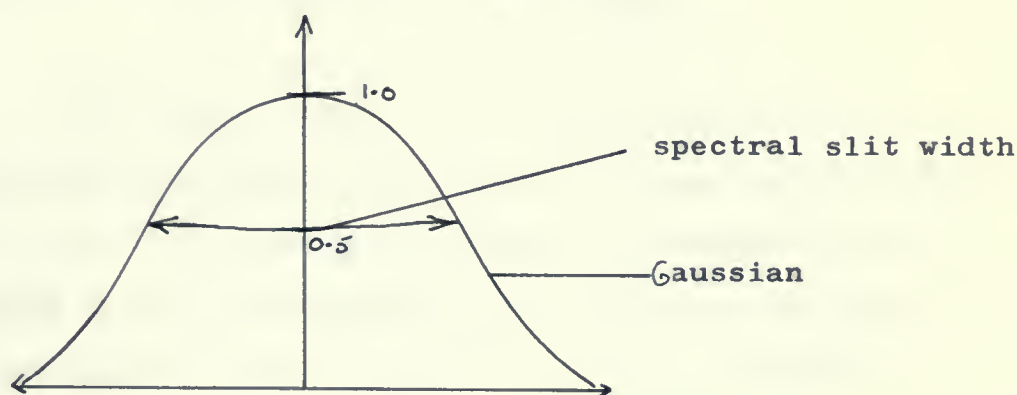


Fig. 2: Relation between Spectral Slit Width and Gaussian.

Actually several types of slit functions such as triangular, Lorentz and square were tried with similar results, but the Gaussian gave the best overall match with experiment.

It is necessary to mention that the spatial width of each frequency component is sufficient to fully illuminate the exit slit, since the entrance slit which was fully illuminated has a width equal or somewhat greater than that of the exit slit.

In the case of infrared, prior to broadening, the scale factor N previously mentioned is determined. To obtain a value of N a small section of the spectrum (peak), is selected by two input frequency boundaries. The scale factor N is calculated so that the final broadened spectra will have the peak absorption

in this region match that of the experimental result. To do this a starting value N_s for N is obtained by forcing the maximum in this range to match the experimental maximum absorption A_m

$$[57a] \quad \text{ie} \quad A_m = (1 - \exp(-S_{i_{\min}} N_s))$$

$$[57b] \quad \therefore N_s = -[\log_e(1 - A_m)]/S_{i_{\min}}$$

Then this small region of the spectrum is converted to absorption and broadened to see if upon broadening the peak absorption is A_m . If it is not N is increased or decreased incrementally according as the peak height was less or greater than A_m . With this new value of N the conversion to absorption and broadening are repeated. The peak height is again compared to A_m ; if required N is again incremented. This process is continued in an iterative fashion until the peak calculated absorption is sufficiently close to A_m . Once this is completed the final spectrum is converted to absorption and broadened.

Photographic or Photoelectric response.

If the experimental spectra are photographically recorded it would be necessary to apply a logarithmic conversion to the broadened spectra. This is necessary to account for the response of the photographic emulsion. In our case we assume photoelectric detection for both infrared and Raman. As a result of this no further transformation need be applied to the infrared, and the Raman intensities need only be scaled between 0 and 100.

(IV-3) Criteria for good comparison between experimental and simulated spectra.

(i) Since the simulation uses a Beers Law type calculation to convert to absorption one must not attempt to compare experimental and computed results where this law does not hold. In practice what this has meant is that the experimentalist should adjust pressure-path length so as to bring the structure of interest between 20-40% absorption. If there are peaks much higher than this then they cannot be reliably compared to calculated results. It is thus clear that the peak chosen for scaling is to be in this range.

(ii) Scan Speed: This is of critical importance as peak heights can be completely changed if the scan is too fast. It goes without saying that the theoretical spectrum is to be compared with an experimental spectrum that was scanned infinitely slowly. In practice this means the scan speed is to be reduced until the spectrum no longer changes with speed reduction. This is to be done with particular regard for peak heights and valley depths. As an example, the experimental infrared spectra presented in this work represent a scan time of approximately eight hours.

(iii) Machine Parameters: It also is obvious that a complete knowledge of all control parameters is critical, since a completely false record may be obtained by improper control settings.

Thus to allow comparison of the computed spectra with other computed or experimental results, certain facts are essential. Some examples are slit convolution, spectral slit width, absorption scale, and scan time if applicable. In the latter where photographic recording is used, scan time does not apply, but the emulsion calibration should be given. Without these basic facts any comparison is not practical and probably meaningless.

Chapter V

RESULTS

The results are in the form of a series of diagrams, each containing two spectra. Diagrams 1 and 2, for CH_3F , are infrared results; the upper spectrum is experimental and the lower a simulation of the same region. The remaining diagrams represent spectra simulated for CD_3Cl . In each diagram the upper assumes no Coriolis coupling and the lower includes this effect.

Each diagram is preceded by a covering page which is a computer print-out of the constants employed. To aid in the interpretation of this print-out, comments are given below.

- (i) The parallel and perpendicular moments represent $\mu_{\parallel}\overline{N_r}$ and $\mu_{\perp}\overline{N_s}$ respectively, as defined in Table IV.
- (ii) In the infrared case a band centre, ν_c , is selected near the centre of the region of investigation. This is used as a scale factor so that the frequency dependence of infrared intensities is given by $\Delta\nu/\nu_c$ rather than $\Delta\nu$, where $\Delta\nu$ is the transition frequency.
- (iii) The frequency in cm^{-1} of the Raman exciting line ν_e is given. This is used as a scale factor so that the frequency dependence of Raman intensities is given by $(\nu_e - \Delta\nu)^4/\nu_e^4$ rather than $(\nu_e - \Delta\nu)^4$.
- (iv) A lower frequency limit in cm^{-1} is given and represents the lower limit of the calculated spectra.
- (v) The frequency step indicates the separation in cm^{-1} of adjacent calculated points in the simulated spectrum.

Note that although all calculations are done with this separation, the final result is plotted in increments (.005") of twice this value due to plotter limitations.

- (vi) The variables ISO, ALPHA02, ALPHA12 and ALPHA22 represent α_0^0 , α_0^2 , α_1^2 and α_2^2 as defined in Table VI.
- (vii) The type of broadening curve applied and the full width at half height of the curve are given.
- (viii) The final four statements refer to the J' and (K'+1) values to which the calculation was done, and the largest accumulated value in the unbroadened relative probability spectra (stick spectra). In the case of an infrared simulation the number of transitions in the spectra are given.

3

...the ... of ...
...the ... of ...
...the ... of ...

...the ... of ...
...the ... of ...
...the ... of ...

...the ... of ...
...the ... of ...
...the ... of ...

...the ... of ...
...the ... of ...
...the ... of ...

...the ... of ...
...the ... of ...
...the ... of ...

...the ... of ...
...the ... of ...
...the ... of ...

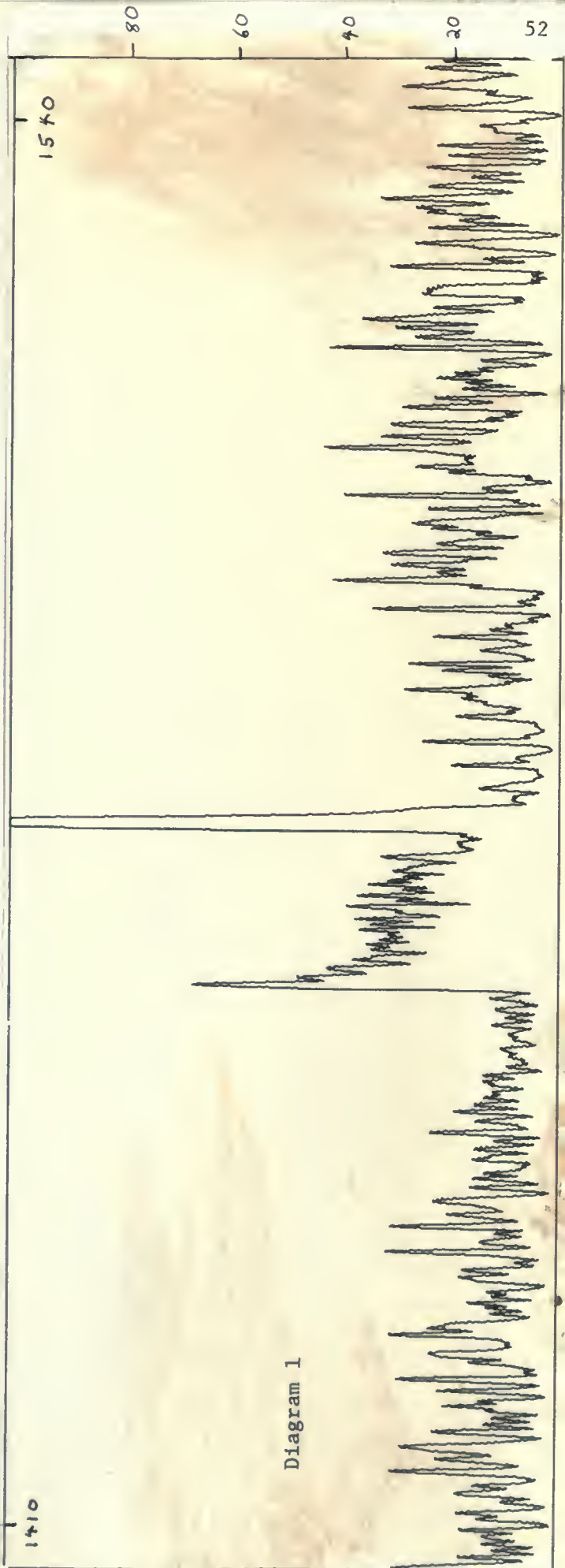
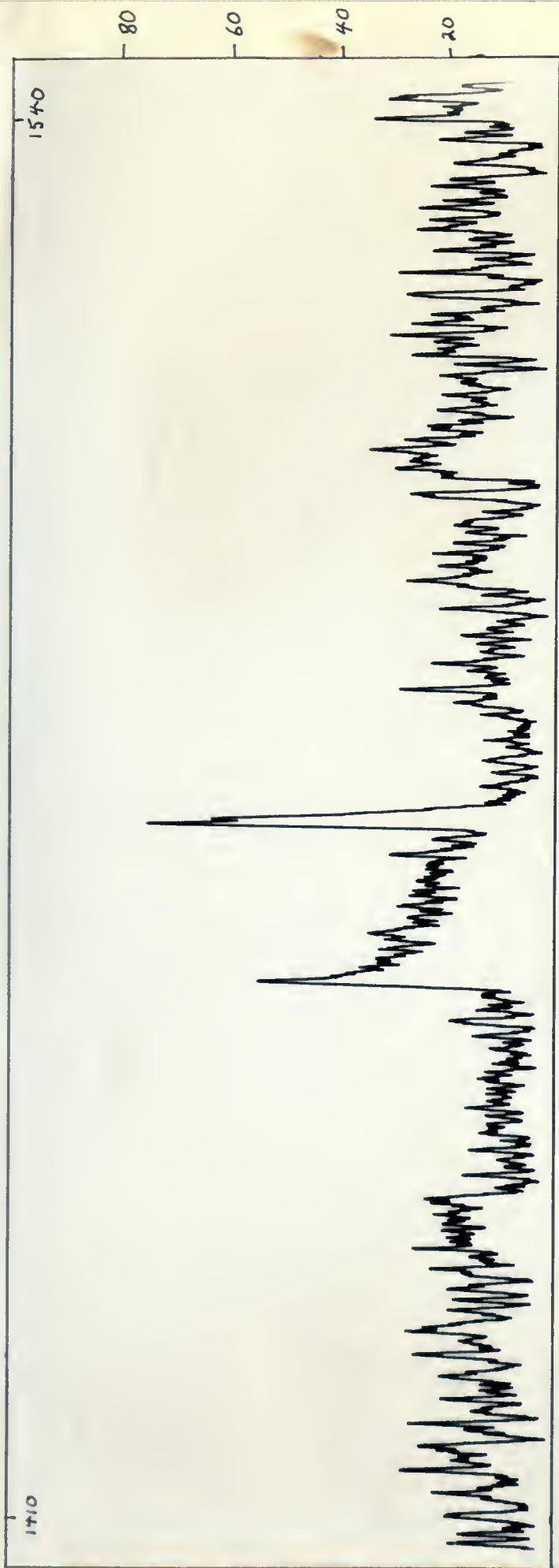

```

#AN INFRARED SPECTRA WAS REQUESTED
#ZETA-X IS INPUTTED AS .6020000
#DEGENERATE UPPER STATE A CONSTANT IS .8571000
#DEGENERATE UPPER STATE B CONSTANT IS .0810000
#NON-DEGENERATE UPPER STATE A CONSTANT IS .8571000
#NON-DEGENERATE UPPER STATE B CONSTANT IS .0810000
#GROUND STATE A CONSTANT IS .8571000
#GROUND STATE B CONSTANT IS .0810000
#NUCLEAR WT. FOR KL NOT A MULTIPLE OF AXIS ORDER IS .20000E+01
#NUCLEAR WT. FOR KL A MULTIPLE OF AXIS ORDER IS .10000E+01
#NUCLEAR WT. FOR K=0 AND JL=0 IS .10000E+01
#NUCLEAR WT. FOR K=1 AND JL=1 IS .10000E+01
#THE PARALLEL TRANSITION MOMENT IS 1.0000000
#THE PERPENDICULAR TRANSITION MOMENT IS 2.3000000
#THE ASSUMED RAND CENTER IS 1465.00000
#THE EXCITING LINE USED WAS 122946.03000
#THE LOWER FREQUENCY LIMIT = 1465.00000
#THE NON-DEGENERATE BAND ORIGIN IS 1467.80000
#THE DEGENERATE BAND ORIGIN IS 1467.80000
#THE FREQUENCY STEP IS 500.00000
#ISO BROADENING IS GAUSSIAN ALPHA2 = .10000E+01 ALPHA22 = .0
#THE HALF WIDTH IS .33000E+01
#THE LARGEST STICK = .91535E-01
#THE LARGEST COEFFICIENT = .12118E+02
#THIS SPECTRUM WAS ABSORPTION SCANNED
#THE WIDTH AT HALF HEIGHT IS .33000
#A(MAXLOC) = .27110E-01 WAVE NO.
#FL = 12118E+02
#A(MAXLOC) = .27110E-01
#FL = .83965E+01
#A(MAXLOC) = .27110E-01
#FL = .7175E+01
#A(MAXLOC) = .27110E-01
#FL = .67364E+01
#A(MAXLOC) = .27110E-01
#FL = .65745E+01
#A(MAXLOC) = .27110E-01
#FL = .55142E+01
#A(MAXLOC) = .27110E-01
#FL = .64916E+01
#THE PEAK ABS COEFF. = .64916E+01
#THE MAXIMUM J VALUE WAS .47000E+02
#THE MAXIMUM K VALUE WAS .49000E+02
#THE NUMBER OF INFRARED TRANSITIONS IS 5547

```

Diagram 1 is Infrared $\nu_2 - \nu_3$ region of CH_3F with $\sqrt{\nu_{\text{H}}}$ = 1 and $\sqrt{\nu_3}$ μ_L = 2.3
 The lower Spectrum is the spectrum simulated with the above constants.

1000






```

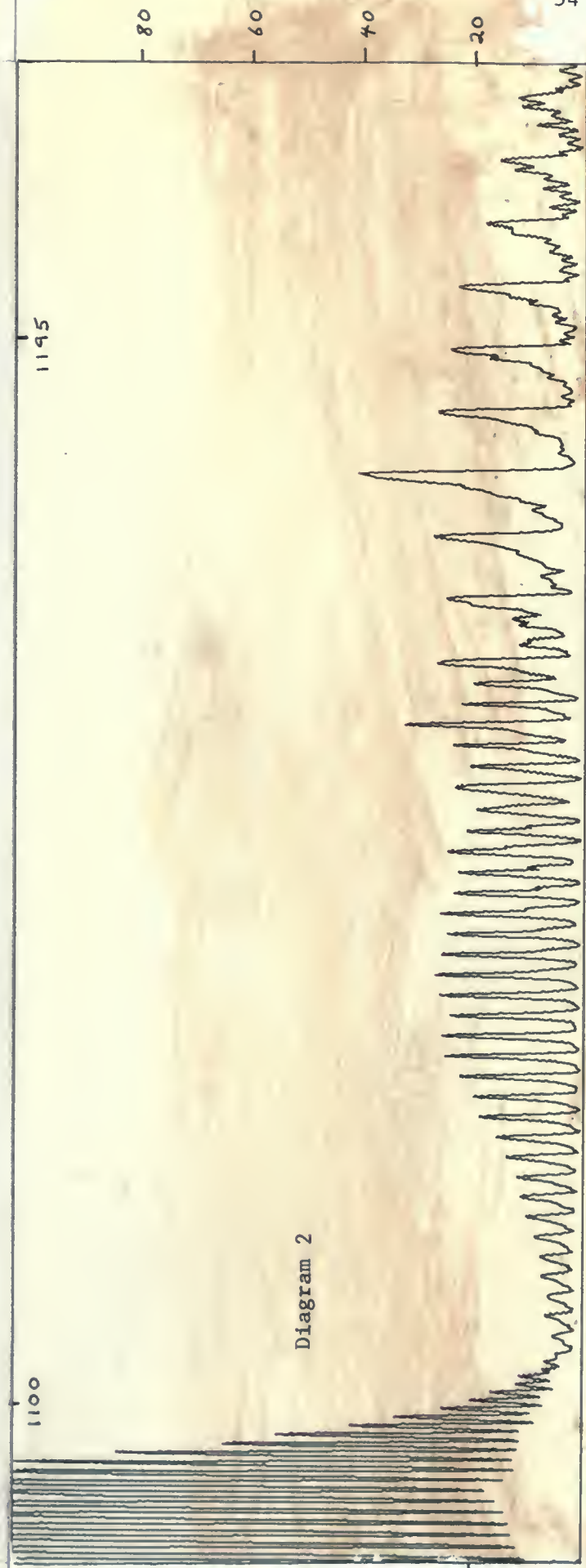
*AN INFRARED SPECTRA WAS REQUESTED
**ZETA-X IS INPUTTED AS -.3180000
**ZETA-Z IS INPUTTED AS .2840000
**DEGENERATE STATE B CONSTANT IS .8484000
**NON-DEGENERATE UPPER STATE A CONSTANT IS .8426000
**NON-DEGENERATE UPPER STATE B CONSTANT IS 5.0697000
**GROUND STATE A CONSTANT IS .8518000
**NUCLEAR WT. FOR K NOT A MULTIPLE OF AXIS ORDER IS .10000E+01
**NUCLEAR WT. FOR K=0 AND J ODD IS .10000E+01
**NUCLEAR WT. FOR K=0 AND J EVEN IS .10000E+01
**THE PARALLEL TRANSITION MOMENT IS 8.4500000
**THE PERPENDICULAR TRANSITION MOMENT IS 1.0000000
**THE EXCITING LINE USED WAS 22946.03051 WAVE NO.
**THE LOWER FREQUENCY LIMIT = .10500E+04
**THE NON-DEGENERATE BAND ORIGIN IS 1048.60000 WAVE NO.
**THE DEGENERATE BAND ORIGIN IS 1182.35000 WAVE NO.
**THE FREQUENCY STEP IS = .5000E-01
**ISCF = -0. ALPHA02 = .10000E+01 ALPHA12 = .10000E+01 ALPHA22 = -0.
**THE BROADENING IS GAUSSIAN
**THE HALF WIDTH IS = .33000E+00
**THE LARGEST STICK = .29789E+01
**THE ABSORPTION COEFFICIENT = .14525E+02
**THIS SPECTRUM WAS ABSORPTION SCANNED
**THE WIDTH AT HALF HEIGHT IS .33000 WAVE NO.
**A(MAXLOC) = .19806E-01
**FL = .14525E+02
**A(MAXLOC) = .57430E-02
**FL = .89442E+01
**A(MAXLOC) = .57430E-02
**FL = .83799E+01
**A(MAXLOC) = .57430E-02
**FL = .83070E+01
**THE PEAK ABS COEFF. = .83070E+01
**THE MAXIMUM J VALUE WAS .48000E+02
**THE MAXIMUM K VALUE WAS .50000E+02
**THE NUMBER OF INFRARED TRANSITIONS IS 5329

```

Diagram 2, Infrared ν_3 - ν_6 region of CH_3F with $\sqrt{\nu_3}\mu_H = 8.45$ and $\sqrt{\nu_6}\mu_L = 1.0$

upper Spectrum experimental, lower spectrum computed.

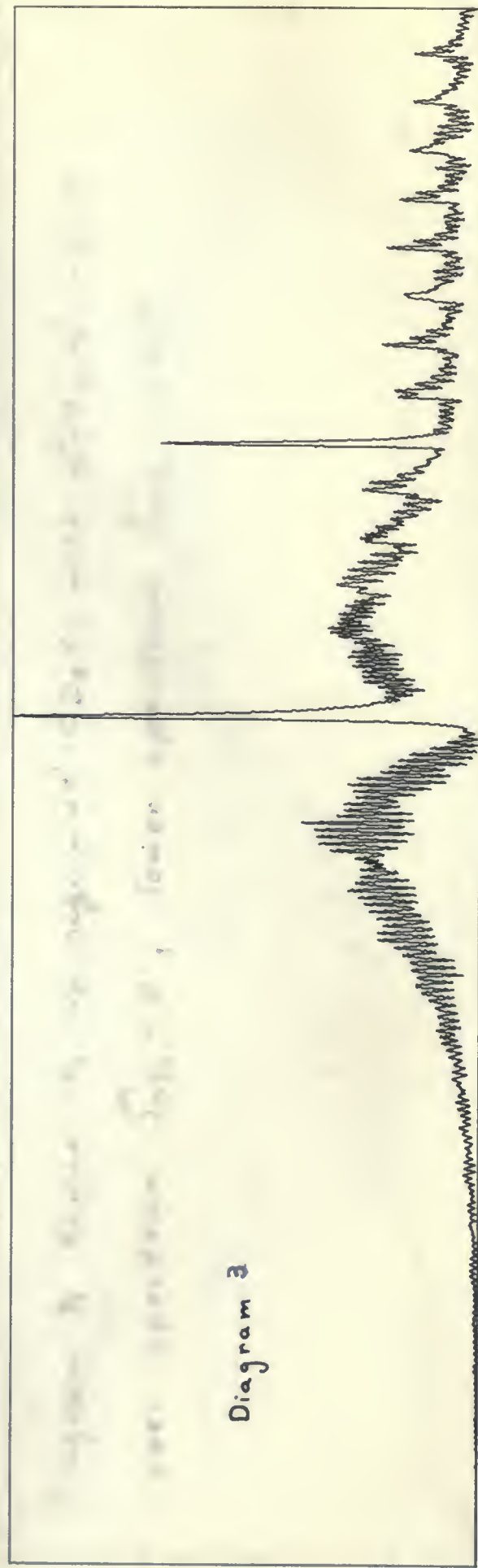
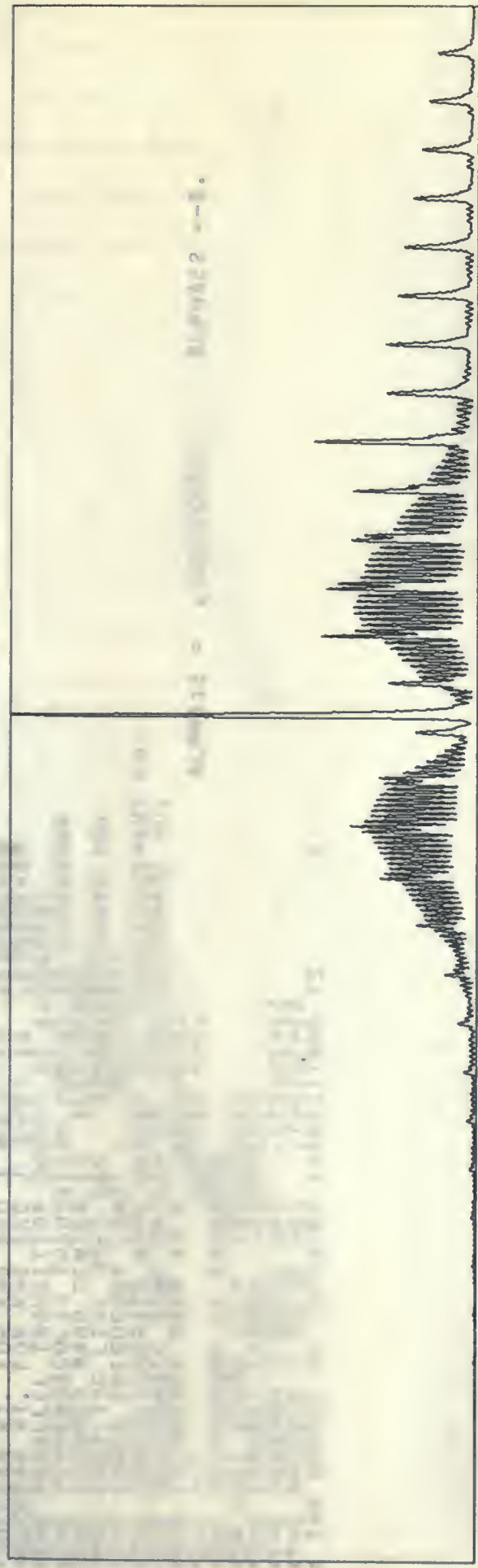




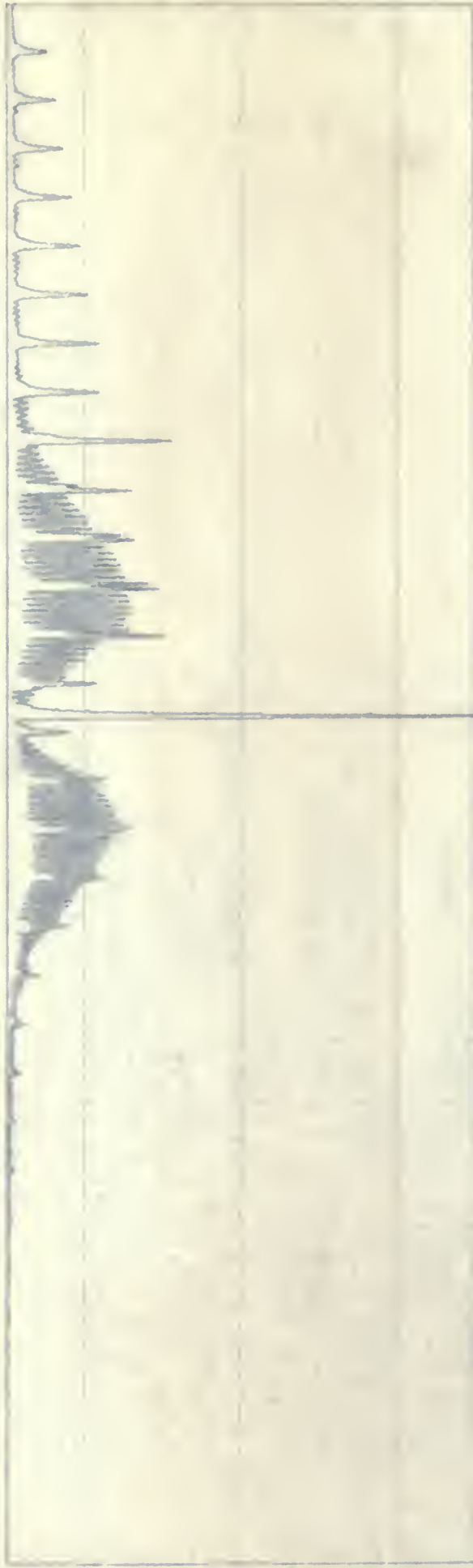


upper spectrum $y^a_{r, y_s} = 0$, lower spectrum $y^a_{r, y_s} = 0.568$





Diagonal



```

#ZETA-X IS INPUTTED AS .56800000
#ZETA-Z IS INPUTTED AS -.33000000
#DEGENERATE STATE B CONSTANT IS .36220000
#DEGENERATE STATE A CONSTANT IS 2.61400000
#NON-DEGENERATE STATE B CONSTANT IS .36226000
#NON-DEGENERATE STATE A CONSTANT IS 2.61400000
#GROUND STATE B CONSTANT IS .36160000
#GROUND STATE A CONSTANT IS 2.61400000
#NUCLEAR WT. FOR K=0 AND J ODD IS .16000000
#NUCLEAR WT. FOR K=0 AND J EVEN IS 1.00000000
#NUCLEAR WT. FOR K=0 AND J ODD IS 1.00000000
#NUCLEAR WT. FOR K=0 AND J EVEN IS 1.00000000
#THE PARALLEL TRANSITION MOMENT IS 1.00000000
#THE ASSUMED BAND CENTER IS 1045.000000
#THE EXCITING LINE USED WAS 2294.603051 WAVE NO.
#THE LOWER FREQUENCY LIMIT = 920000E+03
#THE NON-DEGENERATE BAND ORIGIN IS 1028.720000 WAVE NO.
#THE FREQUENCY STEP IS 50000E-01
#ISO = -0.
#THE BROADENING IS GAUSSIAN
#THE HALF WIDTH IS .500000E+03
#THE LARGEST STICK = .319000E+03
#THE MAXIMUM J VALUE WAS .720000E+02
#THE MAXIMUM K VALUE WAS .740000E+02
#THE NUMBER OF INFRARED TRANSITIONS IS 0
ALPHA12 = .10000E+01 ALPHA22 = -0.

```

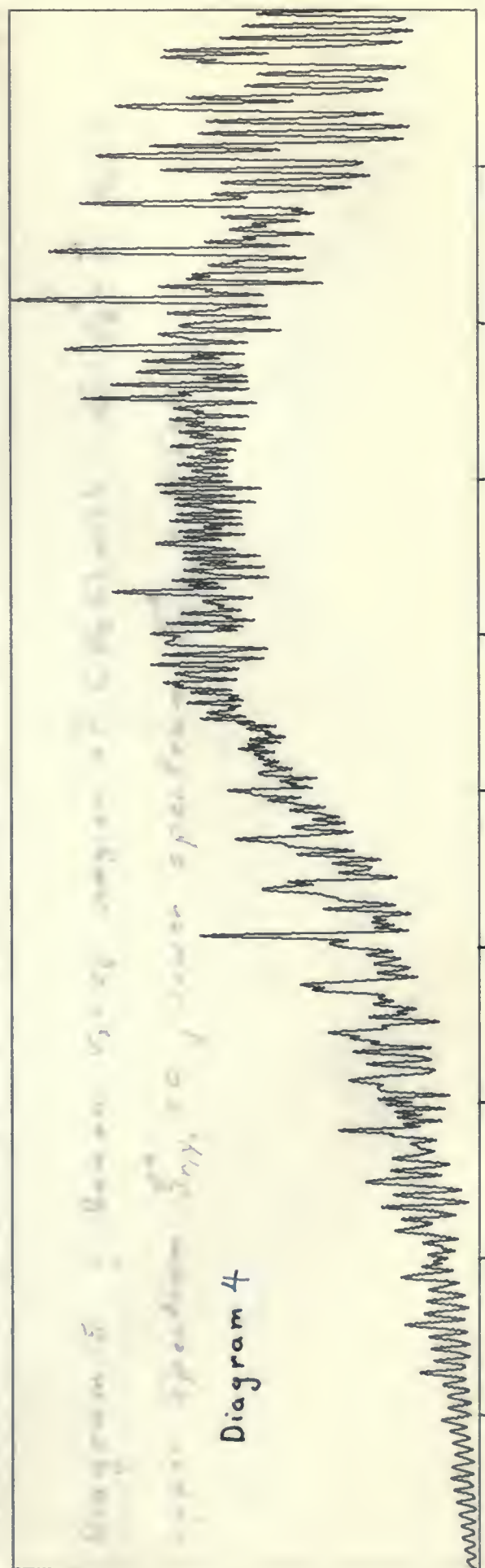
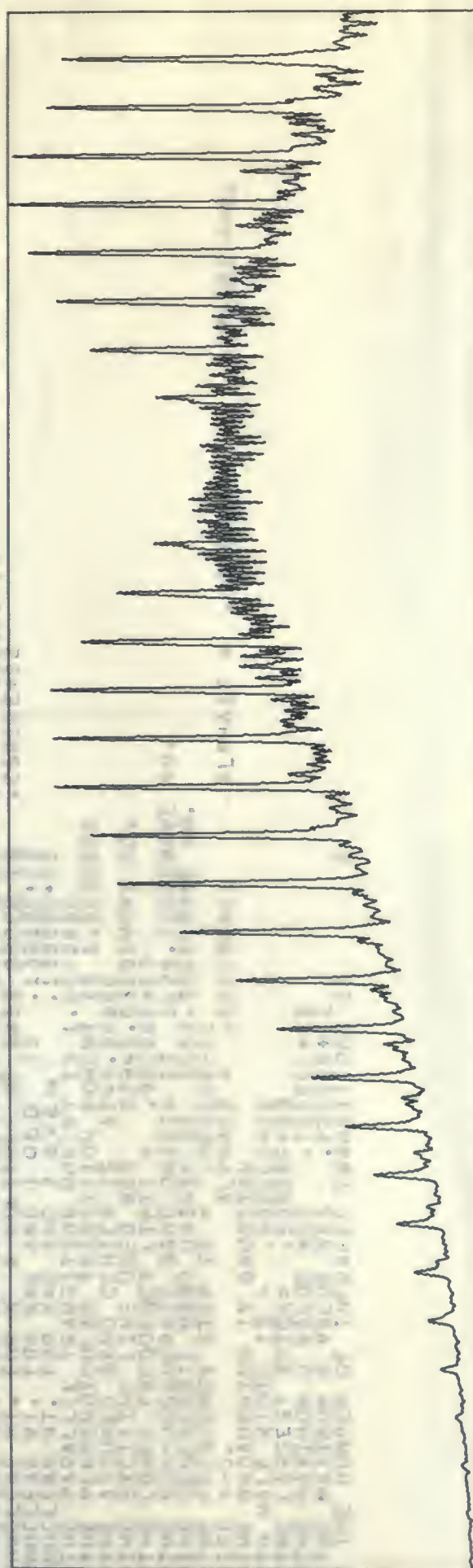
Diagram 4₃ Raman $\nu_2 - \nu_8$ region of CD_3Cl with $\alpha_1^2 = 1$, $\alpha_0^2 = \alpha_2^2 = 0$
 upper spectrum $\sum \gamma_{\nu}^a = 0$, lower spectrum $\sum \gamma_{\nu}^a = 0.568$

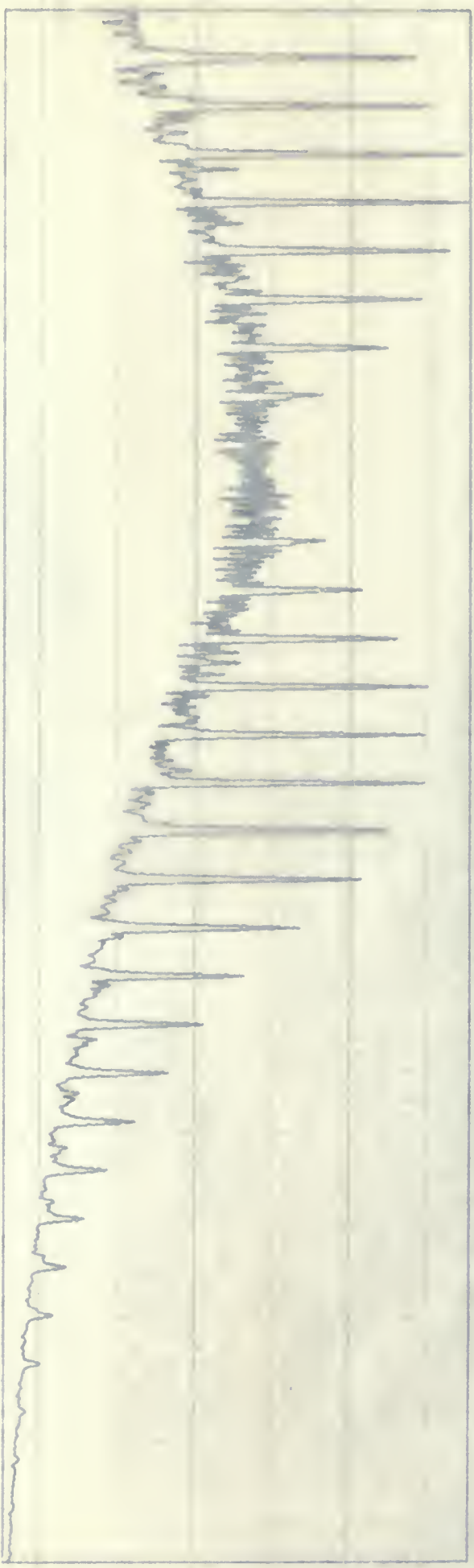
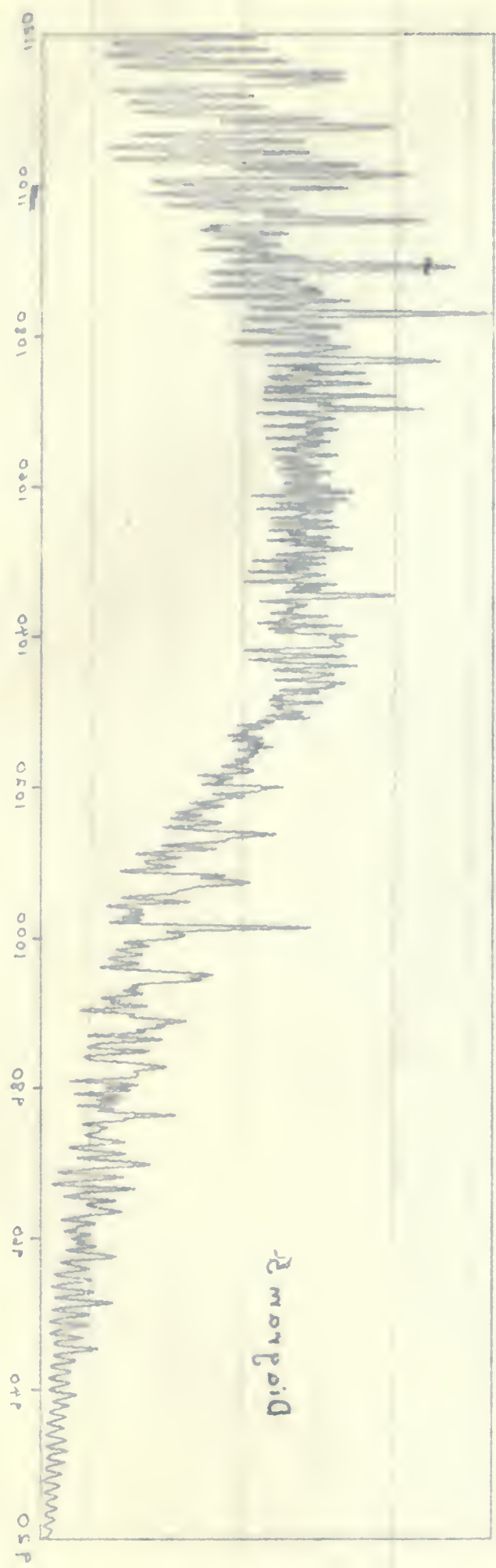
THE UNIVERSITY OF CHICAGO

LIBRARY

1900

1900






```

#ZETA-X IS INPUTTED AS .56800000
#ZETA-Z IS INPUTTED AS -.33000000
#DEGENERATE STATE A CONSTANT IS .3622000
#DEGENERATE STATE B CONSTANT IS 2.6140000
#NON-DEGENERATE UPPER STATE A CONSTANT IS .3626000
#NON-DEGENERATE UPPER STATE B CONSTANT IS 2.6140000
#GROUND STATE A CONSTANT IS .3616000
#GROUND STATE B CONSTANT IS 2.6140000
#NUCLEAR WT. FOR K=0 AND J ODD IS 1.600000
#NUCLEAR WT. FOR K=0 AND J EVEN IS 1.600000
#NUCLEAR WT. FOR K=1 AND J ODD IS 1.600000
#NUCLEAR WT. FOR K=1 AND J EVEN IS 1.600000
#THE PARALLEL BAND CENTRED WAS 22946.03051 WAVE NO.
#THE PERPENDICULAR BAND CENTRED WAS 22946.03051 WAVE NO.
#THE EXCITING FREQUENCY LIMIT = 92000E+03
#THE LOWER FREQUENCY BAND ORIGIN IS 1028.72000 WAVE NO.
#THE NON-DEGENERATE BAND ORIGIN IS 1059.90000 WAVE NO.
#THE FREQUENCY STEP IS = 5000E-01
#ISO = -0.
#THE BROADENING IS GAUSSIAN
#THE HALF WIDTH IS = .5000E+00
#THE LARGEST STICK = .50918E+03
#THE MAXIMUM J VALUE WAS .70000E+02
#THE MAXIMUM K VALUE WAS .72000E+02
#THE NUMBER OF INFRARED TRANSITIONS IS 0

```

ALPHA12 = .10000E+01 ALPHA22 = -0.

Diagram 5 ; Raman $\nu_2 - \nu_6$ region of CD_3Cl with $\alpha_0^2 = \alpha_2^2 = 1$, $\alpha_2^2 = 0$
 upper spectrum $y_a^a = 0$, lower spectrum $y_{r/y_s}^a = 0.568$

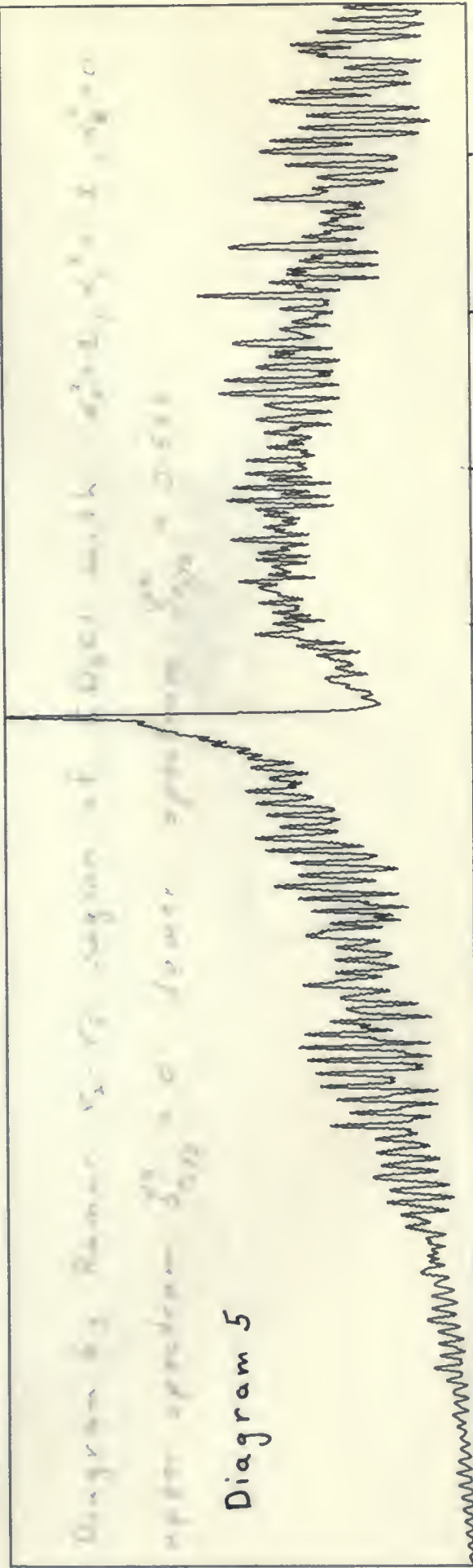
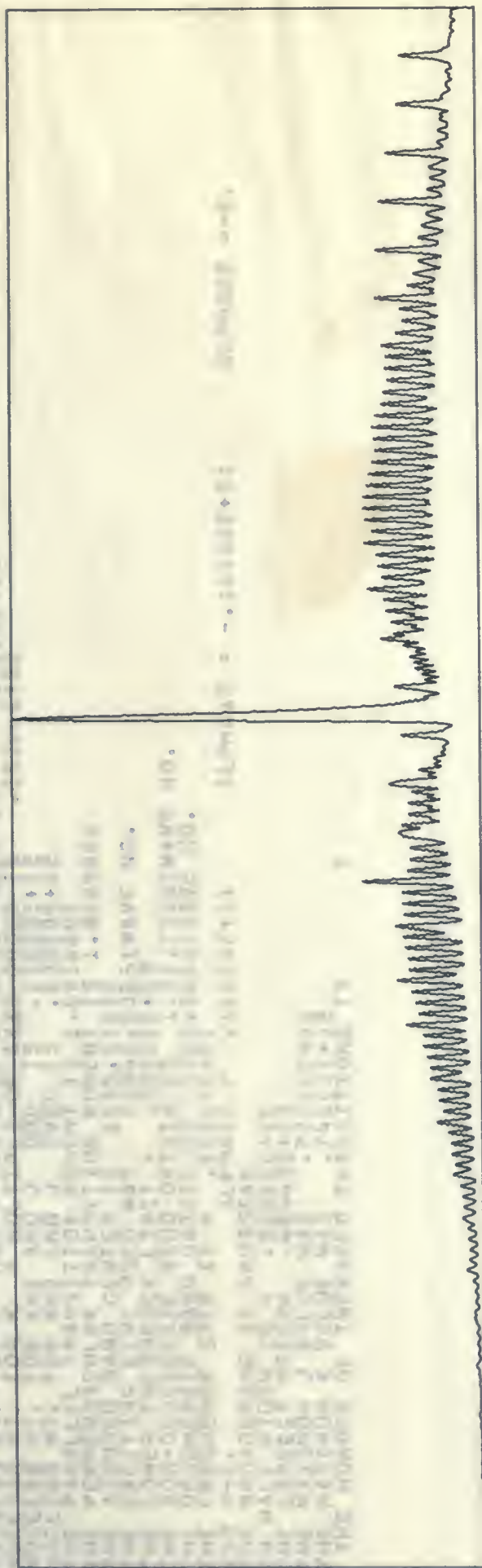
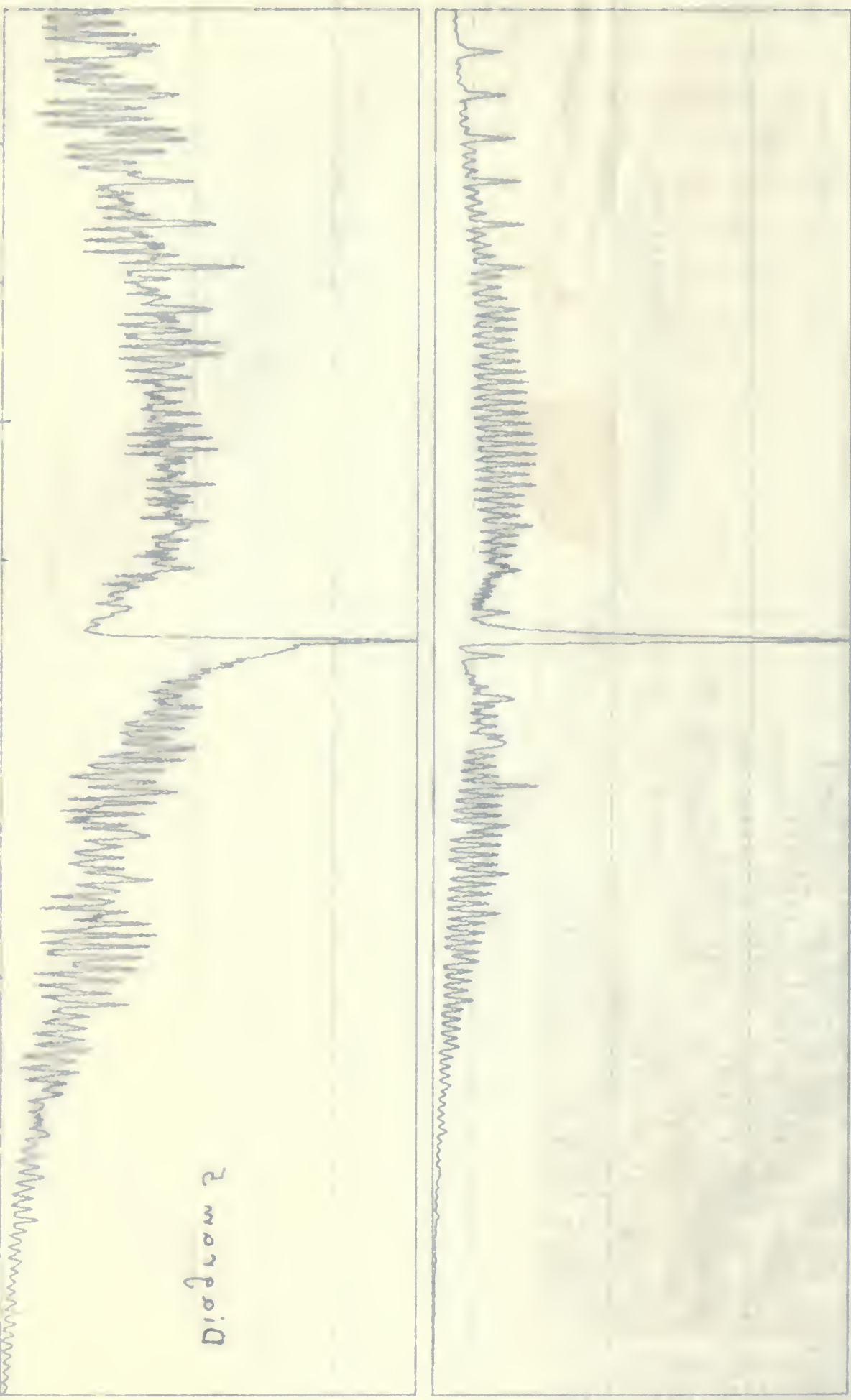


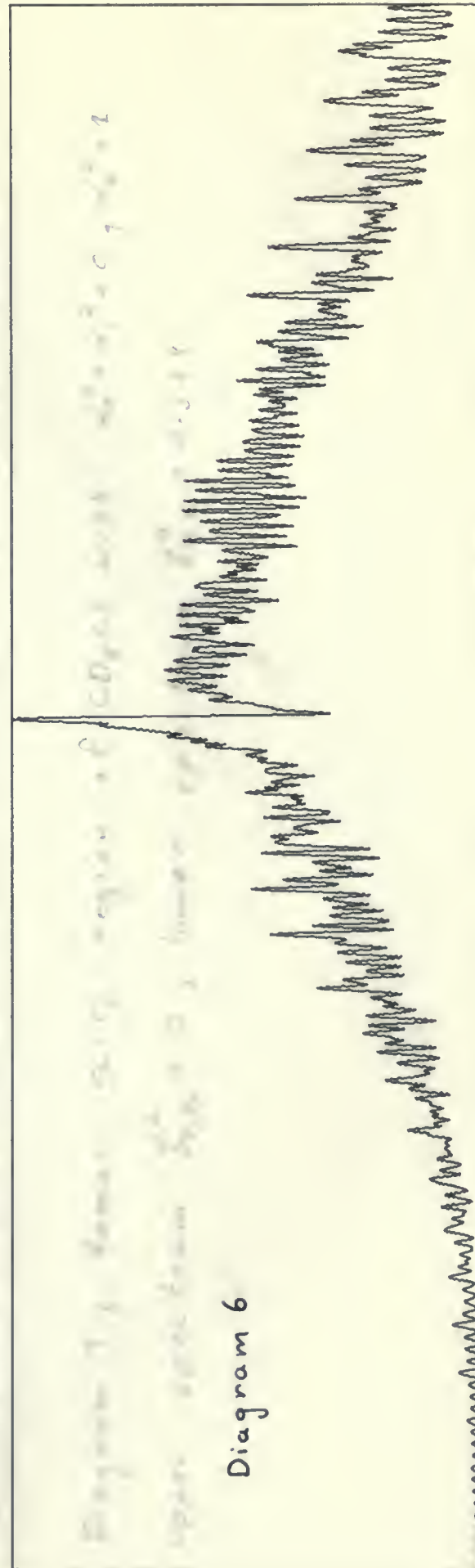
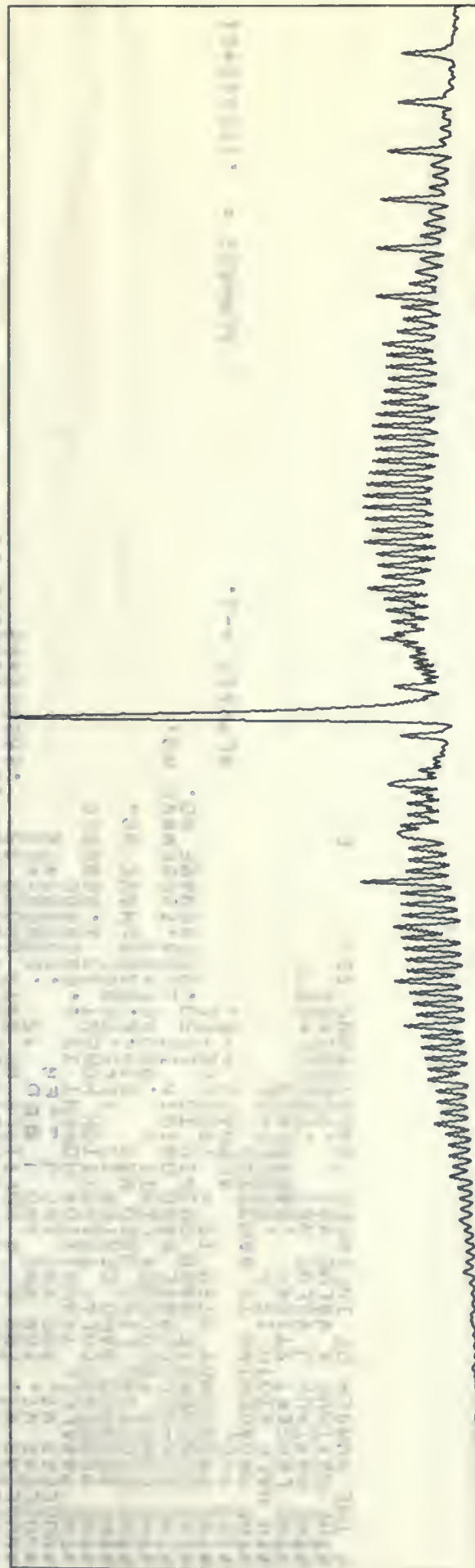
Diagram 5

0511 801 0201 0701 0501 0001 08P 03P 0 050 05P

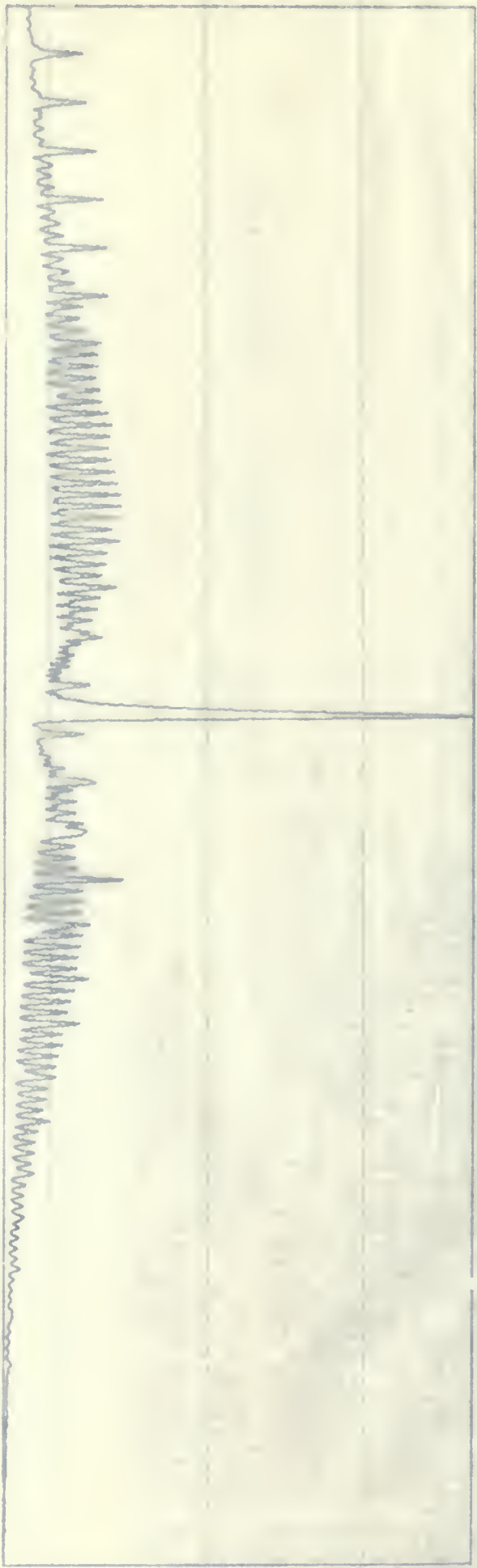
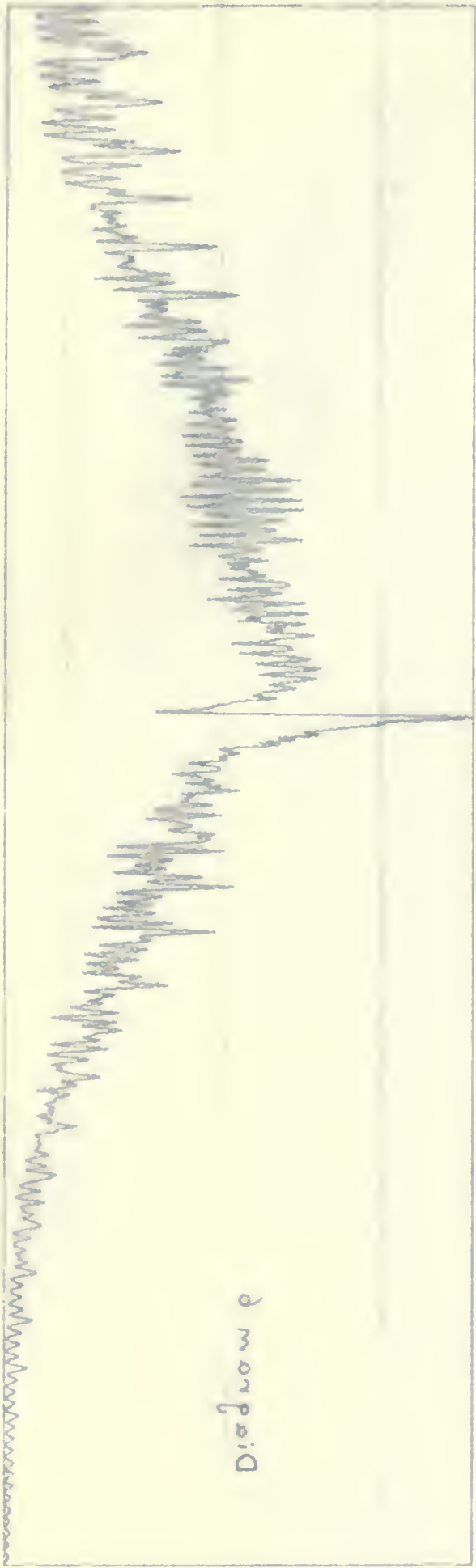
Dispersed







Diagnose




```

ZETA-X IS INPUTTED AS .5681000
ZETA-Z IS INPUTTED AS -.3300000
#ZEGENERATE STATE A CONSTANT IS 2.36220000
#ZEGENERATE STATE B CONSTANT IS 2.6140000
#NON-DEGENERATE STATE A CONSTANT IS .3626000
#NON-DEGENERATE STATE B CONSTANT IS 2.6140000
#GROUND STATE A CONSTANT IS .3616000
#GROUND STATE B CONSTANT IS 2.6140000
#NUCLEAR WT. FOR K=0 AND J ODD IS 1.6000000
#NUCLEAR WT. FOR K=0 AND J EVEN IS 1.0000000
#THE PARALLEL TRANSITION MOMENT IS 1.0000000
#THE PERPENDICULAR TRANSITION MOMENT IS 1.0000000
#THE EXCITING LINE USED WAS 1045.00000
#THE LOWER FREQUENCY LIMIT = 22946.03051 WAVE NO.
#THE NON-DEGENERATE BAND ORIGIN IS 1028.72000 WAVE NO.
#THE FREQUENCY STEP IS 50000E-01
#ISO = -0.
#THE BROADENING IS GAUSSIAN
#THE HALF WIDTH IS 50000E+00
#THE LARGEST STICK = .28897E+03
#THE MAXIMUM J VALUE WAS .72000E+02
#THE MAXIMUM K VALUE WAS .74000E+02
#THE NUMBER OF INFRARED TRANSITIONS IS 0

```

ALPHA12 = -0.

ALPHA22 = .10000E+01

Diagram 7, Raman $\nu_2 - \nu_3$ region of CD_3Cl with $d_0^2 = d_1^2 = 0$, $d_2^2 = 1$

Upper spectrum $y_a^a = 0$, lower spectrum $y_a^a = 0.568$

1811



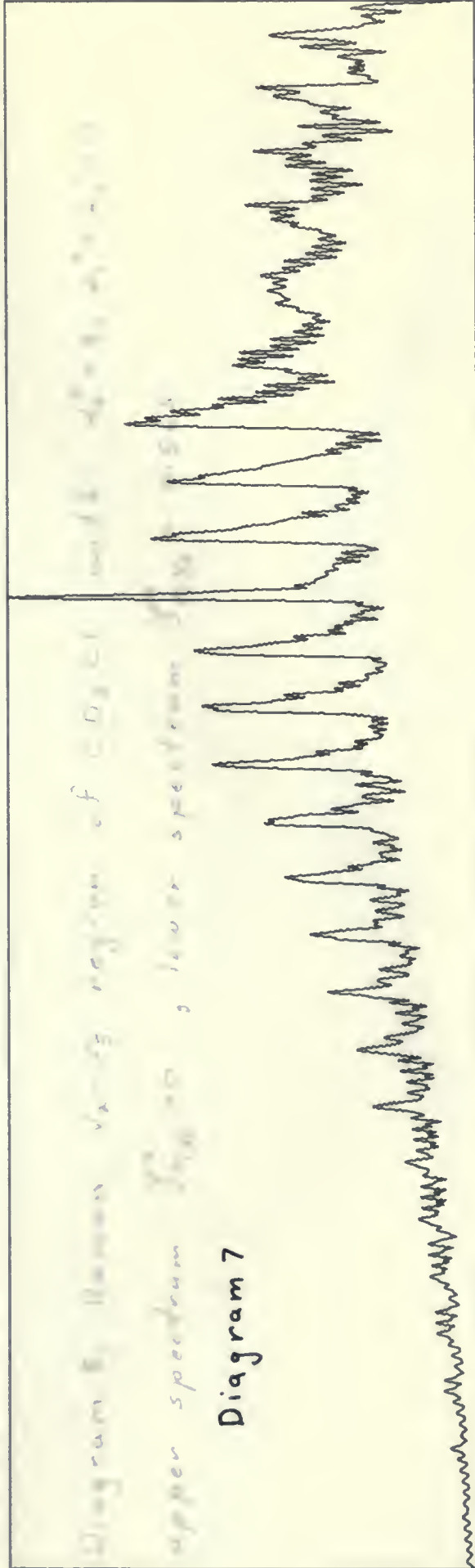
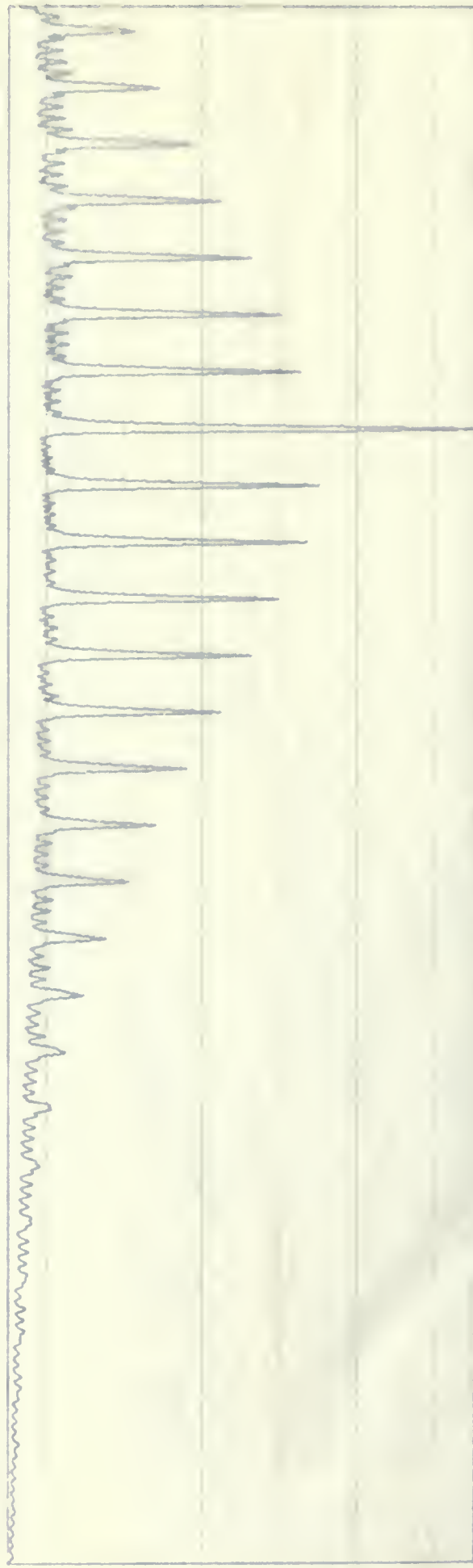
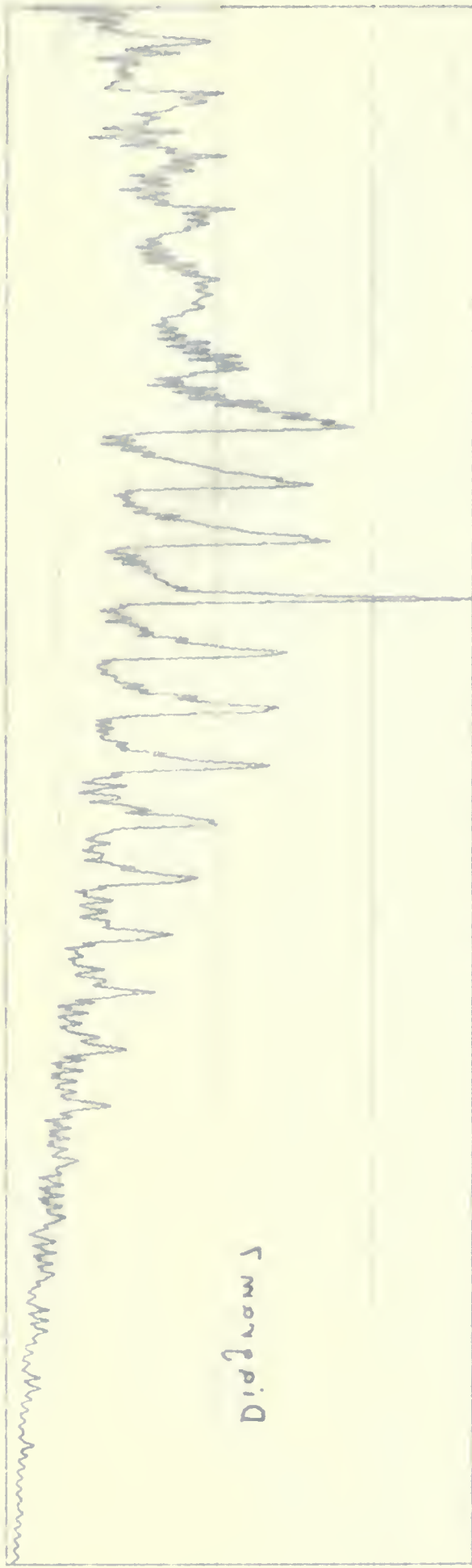


Diagram 7

Dissolved





27480751

SI

1

1

1

1

1

1

1

1

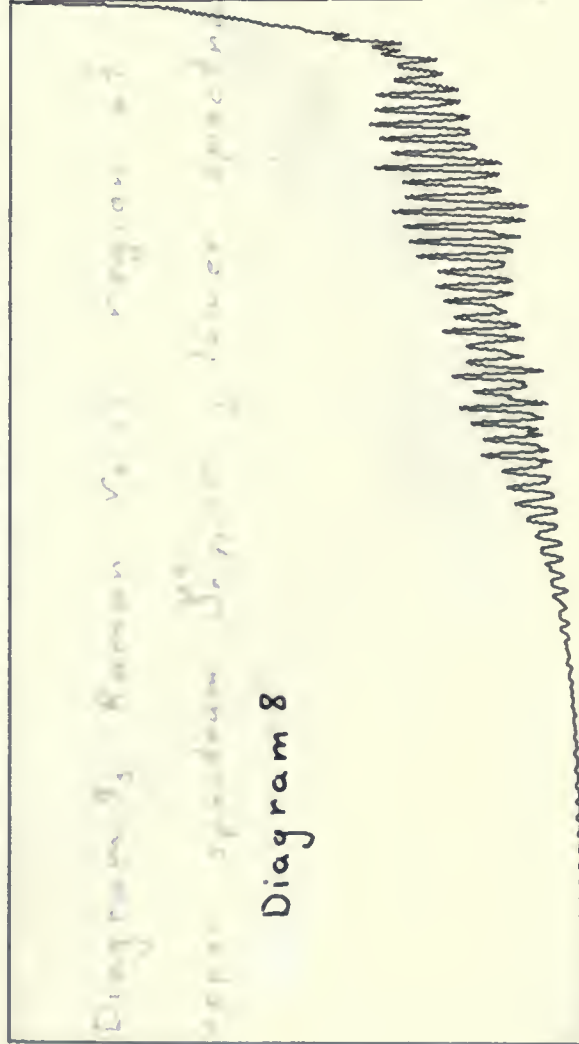
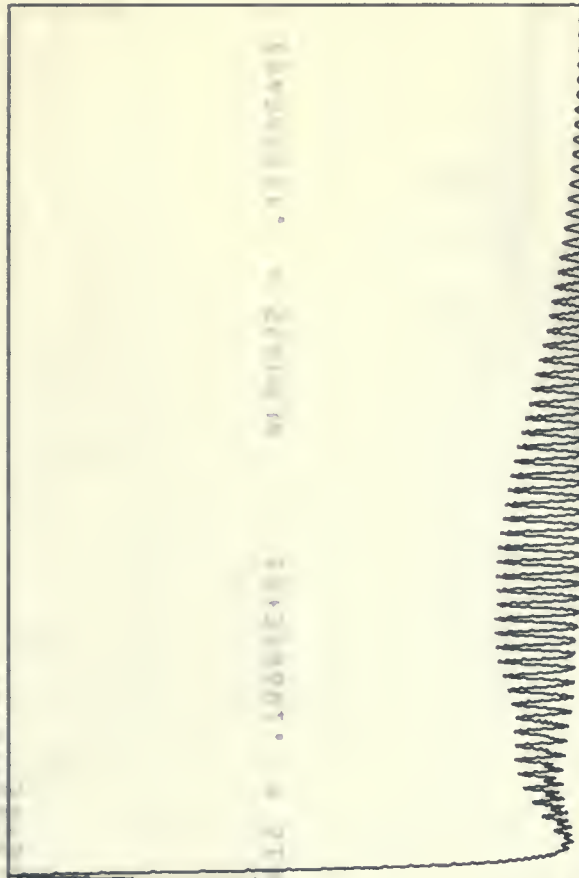
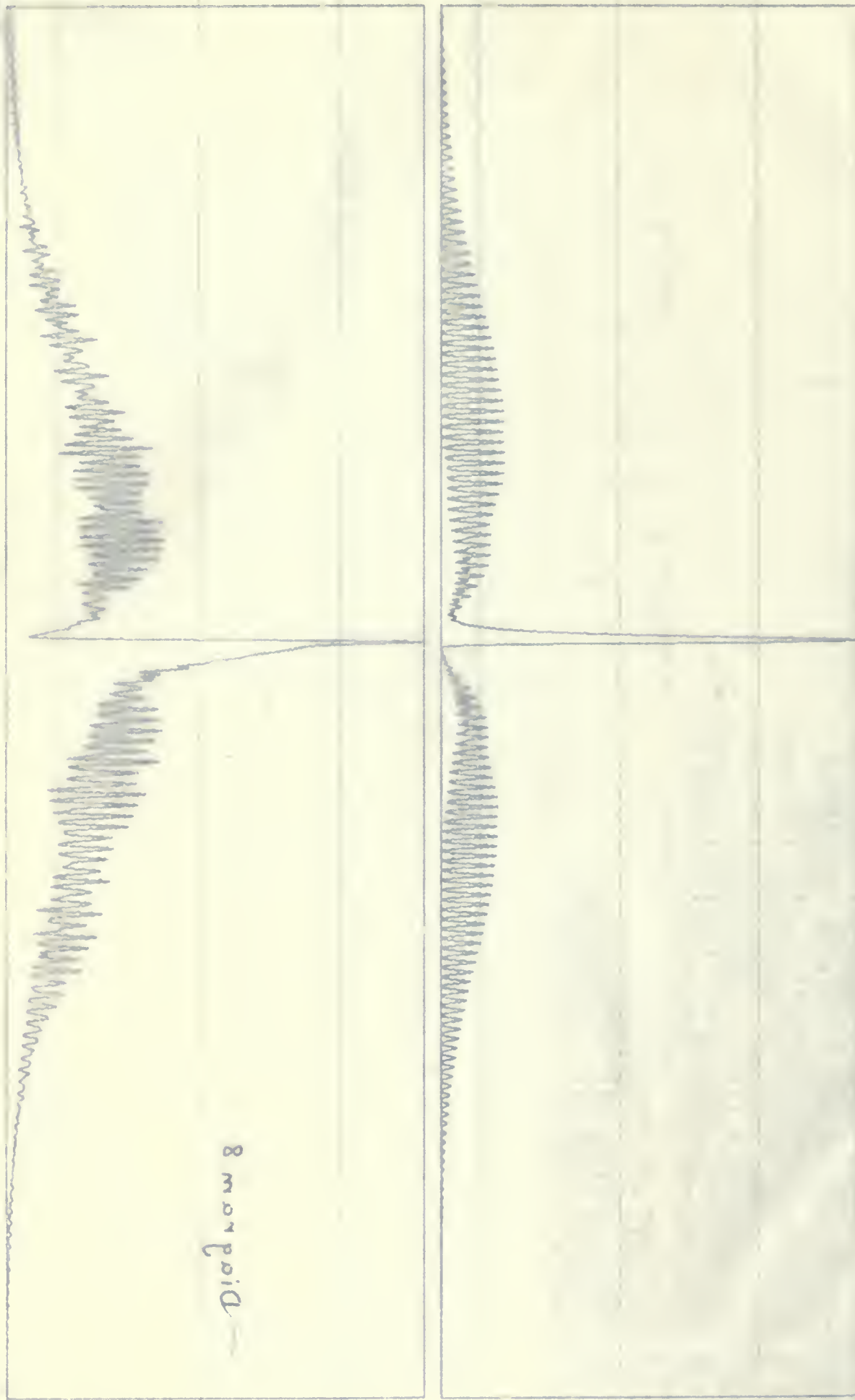


Diagram 8

OSP

0511

8 morpoid




```

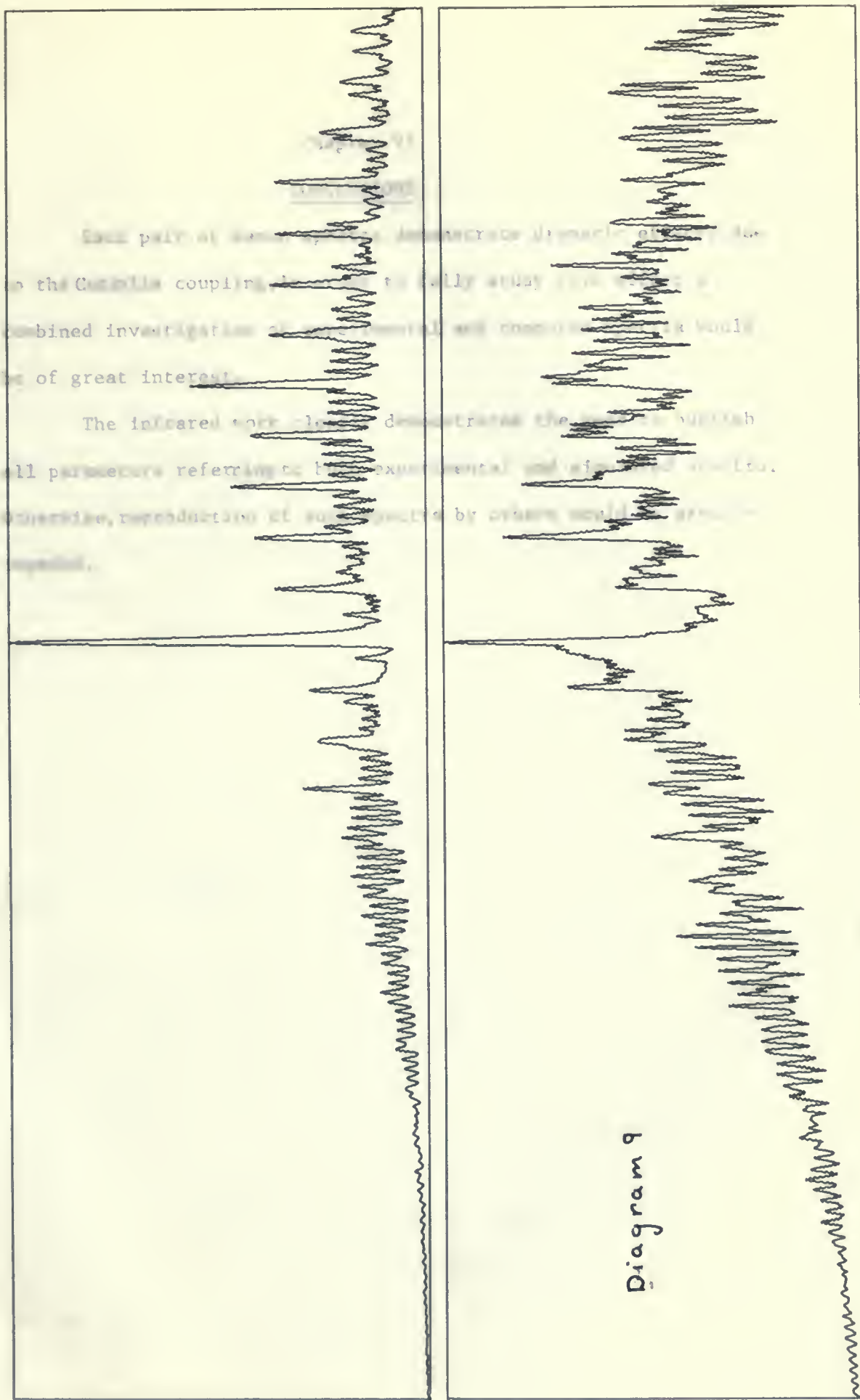
ZETA-X IS INPUTTED AS .5680000
ZETA-Z IS INPUTTED AS -.3300000
DEGENERATE STATE A RATE UPPER STATE IS .3622000
DEGENERATE STATE B RATE UPPER STATE IS 2.6140000
NON-DEGENERATE STATE A CONSTANT IS .3622000
NON-DEGENERATE STATE B CONSTANT IS 2.6140000
GROUND STATE A CONSTANT IS .3622000
GROUND STATE B CONSTANT IS 2.6140000
NUCLEAR WT. FOR K=0 AND J=0 IS .3622000
NUCLEAR WT. FOR K=1 AND J=0 IS .3622000
NUCLEAR WT. FOR K=2 AND J=0 IS .3622000
PARALLEL TRANSITION IS .3622000
PERPENDICULAR TRANSITION IS .3622000
ASSUMED BAND CENTER IS .3622000
EXCITING LINE USED WAS .3622000
LOWER FREQUENCY LIMIT IS .3622000
NON-DEGENERATE BAND ORIGIN IS .3622000
FREQUENCY STEP IS .3622000
ALPHA12 = .10000E+01
ALPHA22 = .10000E+01

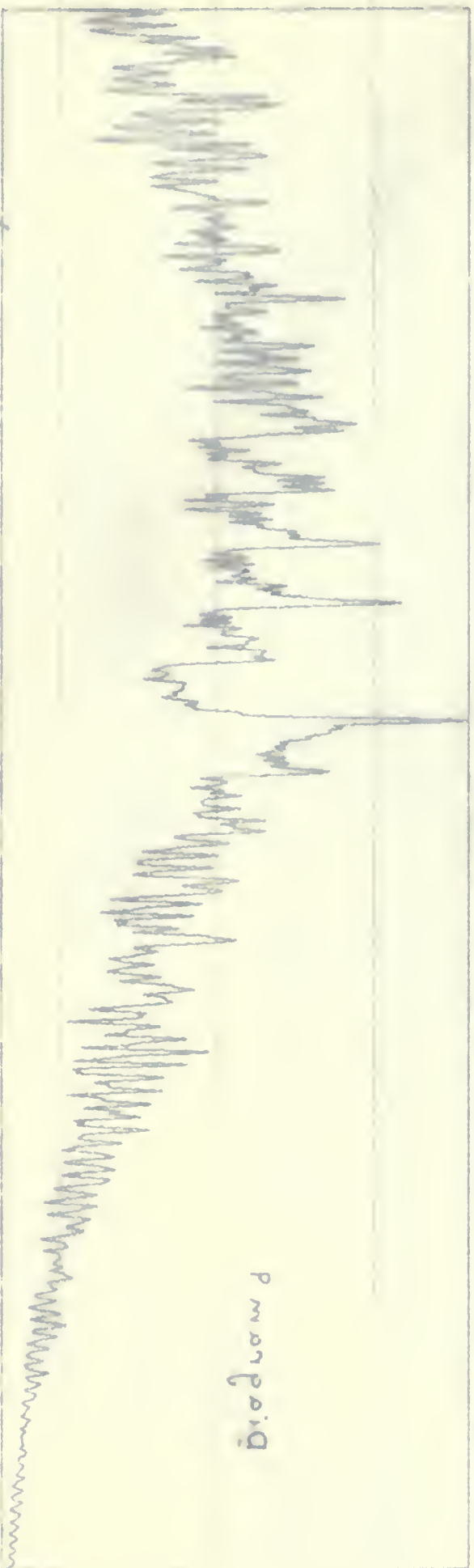
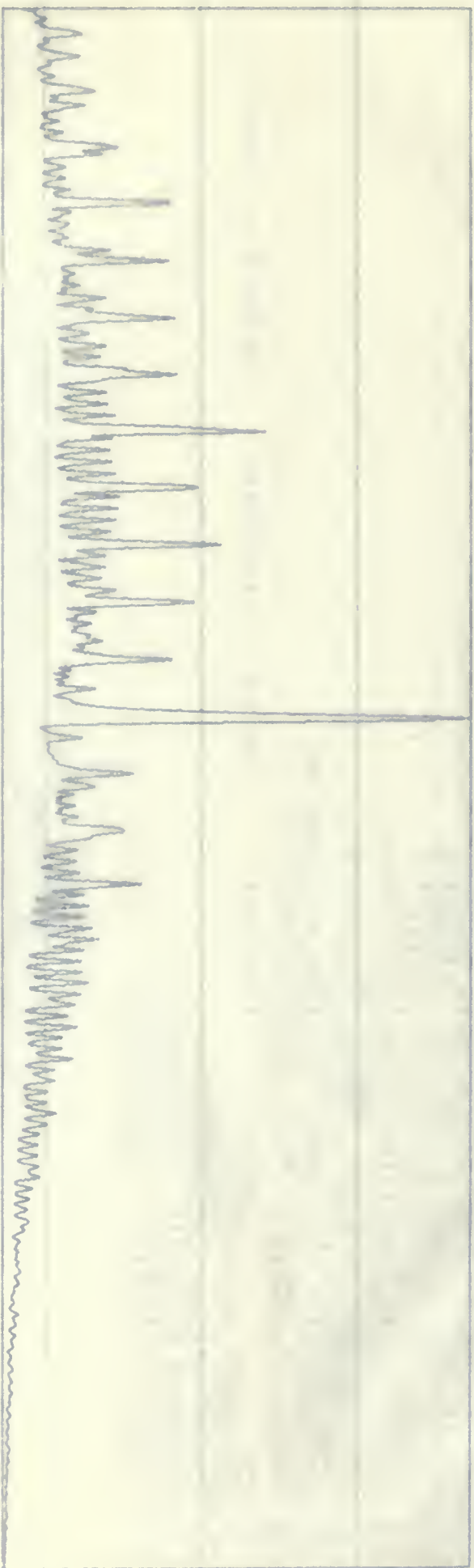
```

Diagram 9, Raman v_2-v_5 region of CD_3Cl with $\lambda_0^2 = \lambda_1^2 = \lambda_2^2 = 1$

upper spectrum y_a , lower spectrum y_b , $y_a = 0.568$







Chapter VI

CONCLUSIONS

Each pair of Raman spectra demonstrate dramatic effects due to the Coriolis coupling. In order to fully study this effect a combined investigation of experimental and computed spectra would be of great interest.

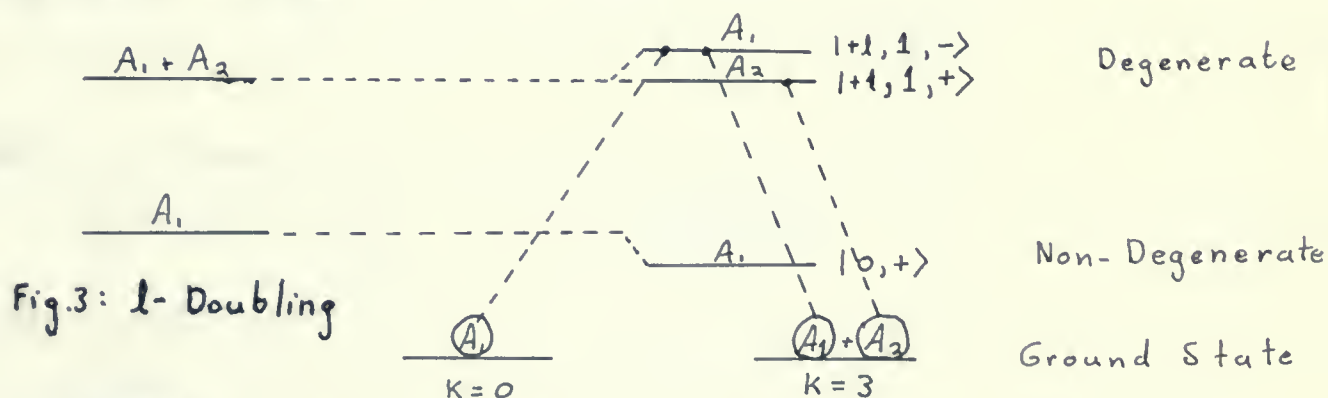
The infrared work clearly demonstrates the need to publish all parameters referring to both experimental and simulated spectra. Otherwise, reproduction of such spectra by others would be greatly impeded.

Appendix I

l - DOUBLING

As an illustration of the complex nature of assigning statistical weights to transitions the following example of l - doubling is cited.

For $K' = 0$ it was stated in (II-4) and illustrated in Table III that the standard 3×3 matrix reduces to a 1×1 and a 2×2 . The 1×1 corresponds to the unshifted $|+1,1,+\rangle$ state and the 2×2 to the interacting $|0,+\rangle$ and $|+1,1,-\rangle$ states. A diagrammatic representation of the effect the coupling has in this case is given below along with the infrared $\Delta k=+1, K=0$ and the Raman $\Delta K=-2, K=3$ transitions.



Note that the coupling interaction splits the $|+1,1,-\rangle$ state from the $|+1,1,+\rangle$ state and the non-degenerate $|0,+\rangle$ state is shifted in the opposite direction. As a result of the doubling of the $|+1,1,+\rangle$ and $|+1,1,-\rangle$ states it is necessary to investigate any possible transitions to these states to be assured that the proper statistical weight is assigned to each such transition. In actual fact the $K=-2, K=3$ Raman transition should have only half the normal weight assigned.

$$\frac{1}{2} \left(\frac{1}{2} + \frac{1}{2} \right) = \frac{1}{2}$$

BIBLIOGRAPHY AND REFERENCES

- ALLEN, H.C., ROSS, P.C.; "Molecular Vib-Rotors", J. Wiley and Sons, New York (1963)
- BLASS, W.E.; Details of First Order Coriolis Resonance in C_{3v} Molecules, J. Mol. Spectroscopy 31, 196-207 (1969)
- BOYD, D.R.J., and LONGUET-HIGGINS, H.C.; Coriolis Interaction between Vibration and Rotation in Symmetric Top Molecules, Proc. Roy. Soc. (London) A213, 55 (1952)
- BREENE Jr., R.G.; Line Width, with figures, "Handbuch der Physik" XVII, pp. 1-79; Springer-Verlag, Berlin (1964)
- CARTWRIGHT, G.J., MILLS, I.M.; ℓ -Resonance Perturbations in Infrared Perpendicular Bands, J. Mol. Spectroscopy, 34, 415 (1970)
- DICKE, R.H., WITTKE, J.P.; "Introduction to Quantum Mechanics", Addison Wesley Publishing Company, Inc. (1960)
- DILAURO, C., MILLS, I.M.; Coriolis Interactions about X-Y Axes in Symmetric Tops, J. Mol. Spectroscopy, 21, 386 (1966)
- DILLING, R.L., PARKER, P.M.; Accidental Coriolis Resonance in Symmetric Top Molecules, J. Mol. Spectroscopy, 22, 178 (1967)
- ELLIS, D.; Ph.D. Thesis, Univ. of Aberdeen, Old Aberdeen, Scotland (1970)
- GARING, J.S., NIELSEN, H.H., RAO, K.N.; The Low-Frequency Vibration Rotation Bands of the Ammonia Molecule, J. Mol. Spectroscopy, 3, 496 (1959)

HERZBERG, G. ; "Infrared and Raman Spectra of Polyatomic Molecules".

D. Van Nostrand Company Inc., New Jersey (1964)

HOUGEN, J.T.; Classification of Rotational Energy Levels for Symmetric-

Top Molecules, J. Chem. Physics, vol. 37, number 7, 1433 (1962)

JONES, E.W., POPPLEWELL, R.J.L., THOMPSON, H.W.; Vibration-rotation

Bands of Methylchloride-d₃, Spectrochimica Acta, vol. 22, 659 (1966)

KIDD, K.G., KING, G.W.; Some Comments on Band Contour Methods, J. Mol.

Spectroscopy, 40, 461 (1971)

KIDD, K.G.; Private Communication

LANDAU, L.D., LIFSHITZ, E.M.; "Quantum Mechanics Non-Relativistic Theory".

Translated to English by J.B. SYKES and J.S. BELL, Pergamon Press,
London (1962)

LEPARD, D.W.; Theoretical Calculations of Electronic Raman Effects of

the NO and O₂ Molecules, Can. J. Physics, Vol. 48, 1664 (1970)

MICHELSON, A.A.; Astrophys. Journal, 2, 251 (1895)

MILLS, I.M., SMITH, W.L., DUNCAN, J.L.; J. Mol. Spectroscopy, 16, 349

(1965)

NIELSEN, H.H.; ℓ -type Doubling in Polyatomic Molecules and its Application

to the Microwave Spectrum of Methylcyanide and Methyl iso-cyanide,

Phys. Rev., 77, 130 (1950)

NIELSEN, H.H.; The Vibration-rotation Energies of Molecules, Rev. Mod. Phys., 23, 90 (1951)

NIELSEN, H.H.; The Vibration-rotation Energies of Molecules and their Spectra in the Infra-red, "Handbuch der Physik" XXXVII/1, p. 170 ff, Springer-Verlag, Berlin (1958)

OKA, T.; Vibration-rotation Interaction in Symmetric-Top Molecules and the Splitting between A_1 and A_2 Levels, J. Chem. Physics, 47, 5410 (1967)

PAULING, L., WILSON, E.B.; "Introduction to Quantum Mechanics with Applications to Chemistry", McGraw-Hill Book Company, Inc., New York (1935)

SMITH, W.L., MILLS, I.M.; Coriolis Perturbations in the Infrared Spectrum of Ethylene, J. Chem. Physics, 40, 2095 (1964)

WATSON, J.K.G.; Simplification of the Molecular Vibration-rotation Hamiltonian, J. Mol. Physics, 15, 479 (1968)

WILSON, E.B., DECIUS, J.C., CROSS, P.C.; "Molecular Vibrations", McGraw-Hill Book Company Inc., New York (1955)

WOLLRAB, J.E. "Rotational Spectra and Molecular Structure", Academic Press, New York (1967)

